
p -Sparsified Sketches for Fast Multiple Output Kernel Methods

Tamim El Ahmad¹ Pierre Laforgue² Florence d’Alché-Buc¹

¹ LTCI, Télécom Paris, Institut Polytechnique de Paris, France

² Department of Computer Science, University of Milan, Italy

Correspondance to: tamim.elahmad@telecom-paris.fr

Abstract

Kernel methods are learning algorithms that enjoy solid theoretical foundations while suffering from important computational limitations. Sketching, that consists in looking for solutions among a subspace of reduced dimension, is a widely studied approach to alleviate this numerical burden. However, fast sketching strategies, such as non-adaptive subsampling, significantly degrade the guarantees of the algorithms, while theoretically-accurate sketches, such as the Gaussian one, turn out to remain relatively slow in practice. In this paper, we introduce the p -sparsified sketches, that combine the benefits from both approaches to achieve a good tradeoff between statistical accuracy and computational efficiency. To support our method, we derive excess risk bounds for both single and multiple output problems, with generic Lipschitz losses, providing new guarantees for a wide range of applications, from robust regression to multiple quantile regression. We also provide empirical evidences of the superiority of our sketches over recent SOTA approaches.

1 Introduction

Kernel methods hold a privileged position in machine learning, as they allow to tackle a large variety of learning tasks in a unique and generic framework, that of Reproducing Kernel Hilbert Spaces (RKHSs), while enjoying solid foundations [66, 61]. From scalar-valued to multiple output regression [53, 17], these approaches play a central role in nonparametric learning, showing a great flexibility. However, when implemented naively, kernel methods raise major issues in terms of time and memory complexity, and are often thought of as limited to “fat data”, i.e., datasets of reduced size but with a large number of input features. One way to scale up kernel methods are the Random Fourier Features [57, 59, 64, 47], but the latter only apply to shift-invariant kernels. Another popular approach is to use sketching methods, first exemplified with Nyström approximations [72, 25, 7]. Indeed, sketching has recently gained a lot of interest in the kernel community due to its wide applicability [75, 43, 40, 42, 30] and its spectacular successes when combined to preconditioners and GPUs [52].

Sketching as a random projection method [49, 73] is rooted in the Johnson-Lindenstrauss lemma [36], and consists in working in reduced dimension subspaces while benefitting from theoretical guarantees. Learning with sketched kernels have mostly been studied in the case of scalar-valued regression, in particular in the emblematic case of Kernel Ridge Regression [3, 6, 75, 20]. For several identified sketches (e.g., Gaussian, Randomized Orthogonal Systems, adaptive subsampling), the resulting estimators come with theoretical guarantees under the form of minimax optimality of the empirical approximation error. However, an important blind spot of the above works is their limitation to the square loss. Few papers go beyond Ridge Regression, and exclusively with subsampling schemes [76, 46, 24]. In this work, we derive excess risk bounds for sketched kernel machines with generic Lipschitz-continuous losses, under standard assumption on the sketch matrix, solving an open problem from [75]. Doing so, we provide theoretical guarantees for a wide range

of applications, from robust regression, based either on the Huber loss [35] or ϵ -insensitive losses [65], to quantile regression, tackled through the minimization of the pinball loss [39]. Furthermore, we address this question in the general context of single and multiple output regression. Learning vector-valued functions using matrix-valued kernels [53] have been primarily motivated by multi-task learning. Although equivalent in functional terms to scalar-valued kernels on pairs of input and tasks [34, Proposition 5], matrix-valued kernels [4] provide a way to define a larger variety of statistical learning problems by distinguishing the role of the inputs from that of the tasks. The computational and memory burden is naturally heavier in multi-task/multi-output regression, as the dimension of the output space plays an inevitable role, making approximation methods for matrix-valued kernel machines a crucial issue. To our knowledge, this work is the first to address this problem under the angle of sketching. It is however worth mentioning the work by [8], who explored spectral filtering approaches to provide efficient implementations of multiple output regression, and a generalization of Random Fourier Features to operator-valued kernels [14].

Another important challenge when sketching kernel methods is that the sketched items, e.g., the Gram matrix, are usually dense. Plain sketches, such as the Gaussian one, then induce significantly more calculations than subsampling methods, which can be computed by applying a mask on the Gram matrix. Motivated by these considerations, we introduce a new family of sketches, the p -sparsified sketches, that achieve interesting tradeoffs between statistical accuracy (Gaussian sketches can be recovered as a particular case of p -sparsified sketches) and computational efficiency. The p -sparsified sketches are also memory-efficient, as they do not require to store the full Gram matrix. Besides a theoretical analysis, we provide extensive experiments showing the superiority of p -sparsified sketches over recent state-of-the-art approaches such as accumulation sketches [20].

Contributions.

- We derive excess risk bounds for both scalar and multiple output sketched kernel machines with generic Lipschitz-continuous loss functions.
- We introduce a new family of sketches, based upon sparse i.i.d. sub-Gaussian entries. It generalizes Gaussian sketches and allows for better computation/accuracy tradeoffs.
- We discuss how to learn these new sketched kernel machines, and present experiments on both synthetic and real-world datasets that support the relevance of our approach.

Notation. For any matrix $A \in \mathbb{R}^{m \times p}$, A^\dagger is its pseudo-inverse, $\|A\|_{\text{op}}$ its operator norm, $A_{i:} \in \mathbb{R}^p$ its i -th row, and $A_{:j} \in \mathbb{R}^m$ its j -th column. The identity matrix of dimension d is I_d . For a random variable $(X, Y) \in \mathcal{X} \times \mathcal{Y}$ with distribution P , P_X is the marginal distribution of X . For $f : \mathcal{X} \rightarrow \mathcal{Y}$, we use $\mathbb{E}[f] = \mathbb{E}_{P_X}[f(X)]$, and $\mathbb{E}[\ell_f] = \mathbb{E}_P[\ell(f(X), Y)]$ for any function $\ell : \mathcal{Y} \times \mathcal{Y} \rightarrow \mathbb{R}$.

2 Sketching Kernels Machines with Lipschitz-Continuous Losses

In this section, we derive excess risk bounds for sketched kernel machines with generic Lipschitz losses. We first focus on scalar regression, before extending our results to multiple output regression.

2.1 Scalar Kernel Machines

We consider a general regression framework, from an input space \mathcal{X} to some scalar output space $\mathcal{Y} \subseteq \mathbb{R}$. Given a loss function $\ell : \mathcal{Y} \times \mathcal{Y} \rightarrow \mathbb{R}$ such that $z \mapsto \ell(z, y)$ is proper, lower semi-continuous and convex for every y , our goal is to estimate $f^* = \arg\inf_{f \in \mathcal{H}} \mathbb{E}_{(X, Y) \sim P}[\ell(f(X), Y)]$, where $\mathcal{H} \subset \mathcal{Y}^{\mathcal{X}}$ is a hypothesis set, and P is a joint probability distribution over $\mathcal{X} \times \mathcal{Y}$. Since P is usually unknown, we assume that we have access to a training dataset $\{(x_i, y_i)\}_{i=1}^n$ composed of i.i.d. realisations drawn from P . We recall the definitions of a scalar-valued kernel and a RKHS [5, 61, 66].

Definition 1 (Scalar-valued kernel). *A scalar-valued kernel is a symmetric function $k : \mathcal{X} \times \mathcal{X} \rightarrow \mathbb{R}$ such that for all $n \in \mathbb{N}$, and any $(x_i)_{i=1}^n \in \mathcal{X}^n$, $(\alpha_i)_{i=1}^n \in \mathbb{R}^n$, we have $\sum_{i,j=1}^n \alpha_i \alpha_j k(x_i, x_j) \geq 0$.*

Any kernel can be uniquely associated to a function space from \mathcal{X} to \mathbb{R} , its RKHS.

Theorem 1 (RKHS). *Let k be a kernel on \mathcal{X} . Then, there exists a unique Hilbert space of functions $\mathcal{H}_k \subset \mathcal{F}(\mathcal{X}, \mathbb{R})$, where $\mathcal{F}(\mathcal{X}, \mathbb{R})$ denotes the set of functions from \mathcal{X} to \mathbb{R} , such that $k(\cdot, x) \in \mathcal{H}_k$ for all $x \in \mathcal{X}$, and such that we have $h(x) = \langle h, k(\cdot, x) \rangle_{\mathcal{H}_k}$ for any $(h, x) \in \mathcal{H}_k \times \mathcal{X}$.*

A kernel machine is an empirical risk minimizer when the hypothesis set is chosen to be a RKHS. It computes a proxy for f^* by solving

$$\min_{f \in \mathcal{H}_k} \frac{1}{n} \sum_{i=1}^n \ell(f(x_i), y_i) + \frac{\lambda}{2} \|f\|_{\mathcal{H}_k}^2, \quad (1)$$

where $\lambda > 0$ is a regularization parameter. By the representer theorem [37], we have that the solution to Problem (1) can be written $\hat{f}_n = \sum_{i=1}^n \hat{\alpha}_i k(\cdot, x_i)$, with $\hat{\alpha} \in \mathbb{R}^n$ the solution to the problem

$$\min_{\alpha \in \mathbb{R}^n} \frac{1}{n} \sum_{i=1}^n \ell([K\alpha]_i, y_i) + \frac{\lambda}{2} \alpha^\top K \alpha, \quad (2)$$

where $K \in \mathbb{R}^{n \times n}$ is the kernel Gram matrix such that $K_{ij} = k(x_i, x_j)$. Given a matrix $S \in \mathbb{R}^{s \times n}$, with $s \ll n$, sketching consists in imposing the substitution $\alpha = S^\top \gamma$. We then obtain an optimisation problem of reduced size on γ , that yields the estimator $\tilde{f}_s = \sum_{i=1}^n [S^\top \tilde{\gamma}]_i k(\cdot, x_i)$, where $\tilde{\gamma} \in \mathbb{R}^s$ is a solution to

$$\min_{\gamma \in \mathbb{R}^s} \frac{1}{n} \sum_{i=1}^n \ell([KS^\top \gamma]_i, y_i) + \frac{\lambda}{2} \gamma^\top S K S^\top \gamma. \quad (3)$$

Works about sketched machines usually assess the performance of \tilde{f}_s either through its squared $L^2(\mathbb{P}_N)$ error $(1/n) \sum_{i=1}^n (\tilde{f}_s(x_i) - f_{\mathcal{H}_k}(x_i))^2$, where $f_{\mathcal{H}_k}$ is the minimizer of the true risk over \mathcal{H}_k , supposed to be attained [75, Equation 2], or through its (relative) recovery error $\|\tilde{f}_s - \hat{f}_n\|_{\mathcal{H}_k} / \|\hat{f}_n\|_{\mathcal{H}_k}$, see [42, Theorem 3]. In contrast, we focus on the excess of risk of \tilde{f}_s for generic Lipschitz losses, as it is the original quantity (i.e., prior to sketching) we want to minimize. As revealed by the proof of Theorem 2, the approximation error term of the excess of risk can be controlled in terms of the $L^2(\mathbb{P}_N)$ error, and we actually recover the results from [75] when we consider the square loss with bounded outputs, see (6). Furthermore, studying the excess of risk allows to better position the performances of \tilde{f}_s among the known off-the-shelf kernel-based estimators available for the targeted problem. To achieve this study, we rely on the key notion of K -satisfiability for a sketch matrix [75, 48, 20].

Let $K/n = UDU^\top$ be the eigendecomposition of the normalized Gram matrix, where $D = \text{diag}(\lambda_1, \dots, \lambda_n)$ stores the eigenvalues of K/n in decreasing order. Let δ_n^2 be the critical radius of K/n , i.e., the lowest value such that $\psi(\delta_n) = (\frac{1}{n} \sum_{i=1}^n \min(\delta_n^2, \lambda_i))^{1/2} \leq \delta_n^2$. The existence and uniqueness of δ_n^2 is guaranteed for any unit ball in the RKHS associated with a positive definite kernel [11, 75]. Note that δ_n^2 is similar to the parameter $\tilde{\varepsilon}^2$ used in [74] for the theoretical analysis of Nyström approximation for kernel methods. Finally, we define the statistical dimension of a Gram matrix as $d_n = \min \{j \in \{1, \dots, n\} : \lambda_j \leq \delta_n^2\}$, with $d_n = n$ if no such index j exists.

Definition 2 (K -satisfiability [75]). *Let $U_1 \in \mathbb{R}^{n \times d_n}$ and $U_2 \in \mathbb{R}^{n \times (n-d_n)}$ be the left and right blocks of matrix U previously defined, and $D_2 = \text{diag}(\lambda_{d_n+1}, \dots, \lambda_n)$. A sketch matrix S is said to be K -satisfiable if there exists a universal constant c such that*

$$\left\| (SU_1)^\top SU_1 - I_{d_n} \right\|_{\text{op}} \leq 1/2, \quad \text{and} \quad \left\| SU_2 D_2^{1/2} \right\|_{\text{op}} \leq c \delta_n. \quad (4)$$

Roughly speaking, a sketch is K -satisfiable if it defines an isometry on the largest eigenvectors of K , and has small operator norm on the smallest eigenvectors. For random sketches, it is common to show K -satisfiability with high probability under some condition on the size s , see e.g., [75, Lemma 5] for Gaussian sketches, [20, Theorem 8] for Accumulation sketches. In Theorem 6, we show similar results for p -sparsified sketches. As in [47], our statistical analysis then relies on the decomposition of the excess of risk as the sum of generalization errors in the RKHS \mathcal{H}_k and an approximation error due to sketching. Bounding the generalization errors requires the following standard assumptions.

Assumption 1. *The true risk is minimized over \mathcal{H}_k at $f_{\mathcal{H}_k} := \arg\inf_{f \in \mathcal{H}_k} \mathbb{E}[\ell(f(X), Y)]$.*

Assumption 2. *For all $y \in \mathcal{Y}$, $z \mapsto \ell(z, y)$ is L -Lipschitz over $\mathcal{H}_k(\mathcal{X}) = \{f(x) : f \in \mathcal{H}_k, x \in \mathcal{X}\}$.*

Assumption 3. *There exists $\kappa > 0$ such that $k(x, x') \leq \kappa$ for all $x, x' \in \mathcal{X}$.*

Assumption 4. *The sketch S is K -satisfiable.*

Note that if Assumption 1 holds, we can reduce the hypothesis set without loss of generality from \mathcal{H}_k to $\{f \in \mathcal{H}_k : \|f\|_{\mathcal{H}_k} \leq \|f_{\mathcal{H}_k}\|_{\mathcal{H}_k}\}$. Up to a rescaling, we may even focus exclusively on $\mathcal{B}(\mathcal{H}_k)$, the unit ball of \mathcal{H}_k [47]. Many loss functions satisfy Assumption 2: for instance, the hinge loss ($L = 1$), used in Support Vector Machines [23], the ϵ -insensitive ℓ_1 [26], the κ -Huber loss, known for robust regression [35], the pinball loss, leveraged in quantile regression [67], or even the square loss with bounded outputs. Assumption 3 is classical and satisfied by many kernels. For instance, it holds for the Gaussian kernel with $\kappa = 1$. Under Assumptions 1 to 4 we have the following result.

Theorem 2. *Suppose that Assumptions 1 to 4 hold, and let $C = 1 + \sqrt{6}c$, with c the universal constant from Assumption 4. Then for any $\delta \in (0, 1)$ with probability at least $1 - \delta$ we have that*

$$\mathbb{E}[\ell_{\tilde{f}_s}] \leq \mathbb{E}[\ell_{f_{\mathcal{H}_k}}] + LC\sqrt{\lambda + \delta_n^2} + 8L\sqrt{\frac{\kappa}{n}} + 2\sqrt{\frac{8\log(2/\delta)}{n}}. \quad (5)$$

Furthermore, if $\ell(z, y) = (z - y)^2/2$ and $\mathcal{Y} \subset [0, 1]$, with probability at least $1 - \delta$ we have that

$$\mathbb{E}[\ell_{\tilde{f}_s}] \leq \mathbb{E}[\ell_{f_{\mathcal{H}_k}}] + C^2(\lambda + \delta_n^2) + 8\frac{\kappa + \sqrt{\kappa}}{\sqrt{n}} + 2\sqrt{\frac{8\log(2/\delta)}{n}}. \quad (6)$$

Proof sketch. The proof relies on the following decomposition of the excess risk

$$\mathbb{E}[\ell_{\tilde{f}_s}] - \mathbb{E}[\ell_{f_{\mathcal{H}_k}}] = \mathbb{E}[\ell_{\tilde{f}_s}] - \mathbb{E}_n[\ell_{\tilde{f}_s}] + \mathbb{E}_n[\ell_{\tilde{f}_s}] - \mathbb{E}_n[\ell_{f_{\mathcal{H}_k}}] + \mathbb{E}_n[\ell_{f_{\mathcal{H}_k}}] - \mathbb{E}[\ell_{f_{\mathcal{H}_k}}]. \quad (7)$$

The two generalization errors (of \tilde{f}_s and $f_{\mathcal{H}_k}$) can be bounded using [12, Theorem 8] together with Assumptions 1 to 3. As for the middle term, we can use Jensen's inequality and the Lipschitz continuity of the loss to upper bound this approximation error by the square root of the sum of the square residuals of the Kernel Ridge Regression with targets the $f_{\mathcal{H}_k}(x_i)$. The latter can in turn be upper bounded using Assumptions 1 and 4 and Lemma 2 from [75]. When we consider the square loss, using Jensen's inequality is not necessary anymore, leading to the improved second term in the r.h.s. of (6). Computing an upper bound on L using that $\mathcal{Y} \subset [0, 1]$ allows to conclude the proof. \square

Bound (5) thus features two different kinds of terms: the quantities related to the generalization errors, expressed in terms of the Rademacher complexity, and a quantity governed by δ_n , deriving from the K -satisfiability analysis. The behaviour of the critical radius δ_n crucially depends on the choice of the kernel. In [75], the authors compute its decay rate for different kernels. For instance, we have $\delta_n^2 = \mathcal{O}(\sqrt{\log(n)}/n)$ for the Gaussian kernel, $\delta_n^2 = \mathcal{O}(1/n)$ for polynomial kernels, or $\delta_n^2 = \mathcal{O}(n^{-2/3})$ for first-order Sobolev kernels. Note that up to the generalization errors, we recover the results derived in [75, Theorem 2] as a particular case of Theorem 2 (with the square loss and bounded outputs). Similarly, by setting $\lambda \propto 1/\sqrt{n}$ we attain a rate of $\mathcal{O}(1/\sqrt{n})$, that is the minimax risk convergence rate for kernel ridge regression, as proved in [15].

Remark 1. *Note that a standard additional assumption on the second order moments of the functions in \mathcal{H}_k [10] allows to derive refined learning rates for the generalization errors in (7). These refined rates are expressed in terms of $\hat{r}_{\mathcal{H}_k}^*$, the fixed point of a new sub-root function $\hat{\psi}_n$. In order to make the approximation error of the same order, it is then necessary to prove the K -satisfiability of S with respect to $\hat{r}_{\mathcal{H}_k}^{*2}$ instead of δ_n^2 . Whether it is possible to prove such a K -satisfiability for standard sketches is however a nontrivial question, that we leave as an interesting research direction for future work. Additional details can be found in Appendix A.2.*

2.2 Matrix-valued Kernel Machines

In this section, we extend our results to multiple output regression, tackled in vector-valued RKHSs. Note that the output space \mathcal{Y} is now a subset of \mathbb{R}^d , with $d \geq 2$. We start by recalling important notions about Operator-Valued Kernels (OVKs) and vector-valued RKHSs (vv-RKHSs) [53, 16, 17, 4].

Definition 3 (Operator-valued kernel). *An OVK is an application $\mathcal{K} : \mathcal{X} \times \mathcal{X} \rightarrow \mathcal{L}(\mathcal{Y})$, where $\mathcal{L}(\mathcal{Y})$ is the set of bounded linear operators on \mathcal{Y} , such that $\mathcal{K}(x, x') = \mathcal{K}(x', x)^\#$ for all $(x, x') \in \mathcal{X}^2$, where $A^\#$ is the adjoint of A , and such that for all $n \in \mathbb{N}$ and any $(x_i, y_i)_{i=1}^n \in (\mathcal{X} \times \mathcal{Y})^n$ we have $\sum_{i,j=1}^n \langle y_i, \mathcal{K}(x_i, x_j) y_j \rangle_{\mathcal{Y}} \geq 0$.*

Like a scalar kernel, an OVK is uniquely associated to a function space from \mathcal{X} to \mathcal{Y} , its vv-RKHS.

Theorem 3 (Vector-valued RKHS). *Let \mathcal{K} be an OVK, and for $x \in \mathcal{X}$, let $\mathcal{K}_x : y \mapsto \mathcal{K}_x y \in \mathcal{F}(\mathcal{X}, \mathcal{Y})$ be the linear operator such that for all $x' \in \mathcal{X}$ we have $(\mathcal{K}_x y)(x') = \mathcal{K}(x', x)y$. Then, there is a unique Hilbert space $\mathcal{H}_{\mathcal{K}} \subset \mathcal{F}(\mathcal{X}, \mathcal{Y})$, the vv-RKHS associated to \mathcal{K} , such that: (i) \mathcal{K}_x spans $\mathcal{H}_{\mathcal{K}}$, i.e., $\mathcal{K}_x y \in \mathcal{H}_{\mathcal{K}}$ for all $y \in \mathcal{Y}$, (ii) \mathcal{K}_x is bounded for the uniform norm for all $x \in \mathcal{X}$, and (iii) we have $f(x) = \mathcal{K}_x^\# f$ for all $f \in \mathcal{H}_{\mathcal{K}}$ and $x \in \mathcal{X}$.*

Note that we focus in this paper on the finite-dimensional case, i.e., $\mathcal{Y} \subset \mathbb{R}^d$, such that for all $x, x' \in \mathcal{X}$, we have $\mathcal{K}(x, x') \in \mathbb{R}^{d \times d}$. For a training sample $\{x_1, \dots, x_n\}$, we define the Gram matrix as $\mathbf{K} = (\mathcal{K}(x_i, x_j))_{1 \leq i, j \leq n} \in \mathbb{R}^{nd \times nd}$. A common assumption then consists in restricting the class of matrix-valued kernels considered to decomposable kernels: we assume that there exist a scalar kernel $k : \mathcal{X} \times \mathcal{X} \rightarrow \mathbb{R}$ and a positive semidefinite matrix $M \in \mathbb{R}^{d \times d}$ such that for all $x, x' \in \mathcal{X}$ we have $\mathcal{K}(x, x') = k(x, x')M$. The Gram matrix can then be written $\mathbf{K} = K \otimes M$, where $K \in \mathbb{R}^{n \times n}$ is the scalar Gram matrix, and \otimes denotes the Kronecker product. Decomposable kernels are widely spread in the literature as they provide a good compromise between computational simplicity and expressivity—in particular they encapsulate independent learning, achieved with $M = I_d$. As in the scalar case, the choice of the matrix-valued kernel, and that of M in particular, plays an important role in learning. We now discuss two examples of relevant output matrices.

Example 1. *In joint quantile regression, one is interested in predicting d different conditional quantiles of an output y given the input x . If $(\tau_i)_{i \leq d} \in (0, 1)$ denote the d different quantile levels, it has been shown in [60] that choosing $M \in \mathbb{R}^{d \times d}$ such that $M_{ij} = \exp(-\gamma(\tau_i - \tau_j)^2)$ favors close predictions for close quantile levels, while limiting the crossing phenomenon.*

Example 2. *In multiple output regression, it is possible to leverage prior knowledge on the task relationships to design a relevant output matrix M . For instance, let P be the $d \times d$ adjacency matrix of a graph in which the vertices are the tasks and an edge exists between task i and j if and only they are (thought to be) related. Denoting by L_P the graph Laplacian associated to P , [27, 62] have proposed to use $M = (\mu L_P + (1 - \mu)I_d)^{-1}$, with $\mu \in [0, 1]$. When $\mu = 0$, we have $M = I_d$ and all tasks are considered independent. When $\mu = 1$, we only rely on the prior knowledge encoded in P .*

Given a training sample $(x_i, y_i)_{i=1}^n \in (\mathcal{X}, \mathbb{R}^d)^n$ and a decomposable kernel $\mathcal{K} = kM$ (its associated vv-RKHS is denoted $\mathcal{H}_{\mathcal{K}}$), the penalized empirical risk minimisation problem is

$$\min_{f \in \mathcal{H}_{\mathcal{K}}} \frac{1}{n} \sum_{i=1}^n \ell(f(x_i), y_i) + \frac{\lambda}{2} \|f\|_{\mathcal{H}_{\mathcal{K}}}^2, \quad (8)$$

where $\ell : \mathbb{R}^d \times \mathbb{R}^d \rightarrow \mathbb{R}$ is a loss function such that $z \mapsto \ell(z, y)$ is proper, lower semi-continuous and convex for all $y \in \mathbb{R}^d$. By the vector-valued representer theorem [53], we have that the solution to Problem (8) writes as $\hat{f}_n = \sum_{j=1}^n \mathcal{K}(\cdot, x_j) \hat{\alpha}_j = \sum_{j=1}^n k(\cdot, x_j) M \hat{\alpha}_j$, where $\hat{A} = (\hat{\alpha}_1, \dots, \hat{\alpha}_n)^\top \in \mathbb{R}^{n \times d}$ is the solution to the problem

$$\min_{A \in \mathbb{R}^{n \times d}} \frac{1}{n} \sum_{i=1}^n \ell([KAM]_{i:}^\top, y_i) + \frac{\lambda}{2} \text{Tr}(KAMA^\top). \quad (9)$$

In this context, performing sketching consists in enforcing the substitution $A = S^\top \Gamma$, where $S \in \mathbb{R}^{s \times n}$ is a sketch matrix and $\Gamma \in \mathbb{R}^{s \times d}$ is the parameter of reduced dimension to be learned. The solution \tilde{f}_s to the sketched problem is then $\tilde{f}_s = \sum_{j=1}^n k(\cdot, x_j) M [S^\top \tilde{\Gamma}]_j$, where $\tilde{\Gamma} = (\tilde{\gamma}_1, \dots, \tilde{\gamma}_s)^\top \in \mathbb{R}^{s \times d}$ is the solution to the sketched problem

$$\min_{\Gamma \in \mathbb{R}^{s \times d}} \frac{1}{n} \sum_{i=1}^n \ell([KS^\top \Gamma M]_{i:}^\top, y_i) + \frac{\lambda}{2} \text{Tr}(KS^\top \Gamma M \Gamma^\top S). \quad (10)$$

Theorem 4. *Suppose that Assumptions 1 to 4 hold, that $\mathcal{K} = kM$ is a decomposable kernel with M invertible, and let C as in Theorem 2. Then for any $\delta \in (0, 1)$ with probability at least $1 - \delta$ we have*

$$\mathbb{E}[\ell_{\tilde{f}_s}] \leq \mathbb{E}[\ell_{f_{\mathcal{H}_{\mathcal{K}}}}] + LC \sqrt{\lambda + \|M\|_{\text{op}} \delta_n^2} + 8L \sqrt{\frac{\kappa \text{Tr}(M)}{n}} + 2 \sqrt{\frac{8 \log(2/\delta)}{n}}. \quad (11)$$

Furthermore, if $\ell(z, y) = \|z - y\|_2^2 / 2$ and $\mathcal{Y} \subset \mathcal{B}(\mathbb{R}^d)$, with probability at least $1 - \delta$ we have that

$$\mathbb{E}[\ell_{\tilde{f}_s}] \leq \mathbb{E}[\ell_{f_{\mathcal{H}_{\mathcal{K}}}}] + C^2 (\lambda + \|M\|_{\text{op}} \delta_n^2) + 8 \text{Tr}(M)^{1/2} \frac{\kappa \|M\|_{\text{op}}^{1/2} + \kappa^{1/2}}{\sqrt{n}} + 2 \sqrt{\frac{8 \log(2/\delta)}{n}}.$$

Proof sketch. The proof follows the same path as that of Theorem 2. The main challenge is to adapt [75, Lemma 2] to the multiple output setting. To do so, we leverage the fact that \mathcal{K} is decomposable, and that S is K -satisfiable, with K the scalar Gram matrix, see Appendix A.3 for technical details. \square

Note that for $M = I_d$ (independent prior), the third term of the r.h.s. of (11) becomes of order $\sqrt{d/n}$, that is typical of multiple output problems. If moreover we instantiate the bound for $d = 1$, we recover exactly Theorem 2. To the best of our knowledge, Theorem 4 is the first theoretical result about sketched vector-valued kernel machines. We again highlight that it applies to generic Lipschitz losses and provides a bound directly on the excess risk, see Appendix B for more details.

2.3 Algorithmic details

We now discuss how to solve Problems (3) and (10). Let $\{(\tilde{\lambda}_i, \tilde{\mathbf{v}}_i), i \in [s]\}$ be the eigenpairs of SKS^\top in descending order, $\tilde{U} = [\tilde{U}_{ij}]_{s \times s} = (\tilde{\mathbf{v}}_1, \dots, \tilde{\mathbf{v}}_s)$, $r = \text{rank}(SKS^\top)$, and $\tilde{K}_r = \tilde{U}_r \tilde{D}_r^{-1/2}$, where $\tilde{D}_r = \text{diag}(\tilde{\lambda}_1, \dots, \tilde{\lambda}_r)$, and $\tilde{U}_r = (\tilde{\mathbf{v}}_1, \dots, \tilde{\mathbf{v}}_r)$. We have the next result.

Proposition 5. *Solving Problem (3) is equivalent to solving the following feature map problem*

$$\min_{\omega \in \mathbb{R}^r} \frac{1}{n} \sum_{i=1}^n \ell(\omega^\top \mathbf{z}_S(x_i), y_i) + \frac{\lambda}{2} \|\omega\|_2^2, \quad (12)$$

where $\mathbf{z}_S(x) = \tilde{K}_r^\top S(k(x, x_1), \dots, k(x, x_n))^\top \in \mathbb{R}^r$.

Problem (12) thus writes as a linear problem with respect to the feature maps induced by the sketch, generalizing the results established in [74] for sub-sampling sketches. When turning to multiple outputs, it is also possible to derive a linear feature map version of Problem (10) when the kernel is decomposable. These feature maps are of the form $\mathbf{z}_S \otimes M^{1/2}$, yielding matrices of size $nd \times rd$ that are prohibitive in terms of space, see Appendix D. Note that an alternative way is to see sketching as a projection of the $k(\cdot, x_i)$ into \mathbb{R}^r [19]. Instead, we directly tackle Problem (10) and learn Γ . For both Problems (3) and (10), we consider losses not differentiable everywhere in Section 4 and apply ADAM Stochastic Subgradient Descent [38] for its efficiency and its ability to handle large datasets.

Remark 2. *In the previous sections, sketching is always leveraged in primal problems. However, for some of the loss functions we consider, dual problems are usually more attractive [23, 44]. This naturally raises the question of investigating the interplay between sketching and duality on the algorithmic level. Due to space limitations, this discussion is postponed to Appendix E.*

3 p -Sparsified Sketches

We now introduce the p -sparsified sketches, and establish their K -satisfiability. The p -sparsified sketches are composed of i.i.d. Rademacher or centered Gaussian entries, multiplied by independent Bernoulli variables of parameter p (the non-zero entries are scaled to ensure that S defines an isometry in expectation). The sketch sparsity is controlled by p , and when the latter becomes small enough, S contains a lot of columns full of zeros. It is then possible to rewrite S as the product of a sub-Gaussian and a subsampling sketch of reduced size, which greatly accelerates the computations.

Definition 4. *Let $s < n$, and $p \in (0, 1]$. A p -Sparsified Rademacher (p -SR) sketch is a random matrix $S \in \mathbb{R}^{s \times n}$ whose entries S_{ij} are independent and identically distributed (i.i.d.) as follows*

$$S_{ij} = \begin{cases} \frac{1}{\sqrt{sp}} & \text{with probability } \frac{p}{2} \\ 0 & \text{with probability } 1 - p \\ \frac{-1}{\sqrt{sp}} & \text{with probability } \frac{p}{2} \end{cases} \quad (13)$$

A p -Sparsified Gaussian (p -SG) sketch is a random matrix $S \in \mathbb{R}^{s \times n}$ whose entries S_{ij} are i.i.d. as follows

$$S_{ij} = \begin{cases} \frac{1}{\sqrt{sp}} G_{ij} & \text{with probability } p \\ 0 & \text{with probability } 1 - p \end{cases} \quad (14)$$

where the G_{ij} are i.i.d. standard normal random variables. Note that standard Gaussian sketches are a special case of p -SG sketches, corresponding to $p = 1$.

Several works partially addressed p -SR sketches in the past literature. For instance, [9] establish that p -SR sketches satisfy the Restricted Isometry Property (based on concentration results from [1]), but only for $p = 1$ and $p = 1/3$. In [45], the authors consider generic p -SR sketches, but do not provide any theoretical result outside of a moment analysis. As far as we know, this is the first time p -SG sketches are introduced in the literature. Note that both (13) and (14) can be rewritten as $S_{ij} = (1/\sqrt{sp})B_{ij}R_{ij}$, where the B_{ij} are i.i.d. Bernoulli random variables of parameter p , and the R_{ij} are i.i.d. random variables, independent from the B_{ij} , such that $\mathbb{E}[R_{ij}] = 0$ and $\mathbb{E}[R_{ij}R_{i'j'}] = 1$ if $i = i'$ and $j = j'$, and 0 otherwise. Namely, for p -SG sketches $R_{ij} = G_{ij}$ is a standard Gaussian variable while for p -SR sketches it is a Rademacher random variable. It is then easy to check that p -SR and p -SG sketches define isometries in expectation, i.e., for all $x \in \mathbb{R}^n$ we have $\mathbb{E}[\|Sx\|_2^2] = \|x\|_2^2$.

Computational efficiency of p -sparsified sketches compared to standard sketches. The main quantity to compute when sketching a kernel machine is the matrix SKS^\top . With standard Gaussian sketches, that are known to be theoretically accurate, this computation takes $\mathcal{O}(sn^2)$ operations. Subsampling sketches are notoriously less precise, but since they act as masks over the Gram matrix K , computing SKS^\top can be done in $\mathcal{O}(s^2)$ operations only. Now, let $S \in \mathbb{R}^{s \times n}$ be a p -sparsified sketch, and $n - s' = s_0(S) = \sum_{j=1}^n \mathbb{I}\{S_{:j} = 0_s\}$ be the number of columns of S full of zeros. The crucial observation that makes S computationally efficient is that we have

$$S = S_{\text{SG}} S_{\text{SS}}, \quad (15)$$

where $S_{\text{SG}} \in \mathbb{R}^{s \times s'}$ is obtained by deleting the null columns from S , and $S_{\text{SS}} \in \mathbb{R}^{s' \times n}$ is a sub-Sampling sketch whose sampling indices correspond to the indices of the columns in S with at least one non-zero entry¹. Note that s' is a random variable, whose distribution only depends on n , s , and p . Indeed, by the independence of the entries, each column is null with probability $(1 - p)^s$, and by the independence of the columns, s' follows a Binomial distribution of parameters n and $1 - (1 - p)^s$, such that we have $\mathbb{E}[s'] = n(1 - (1 - p)^s)$. Decomposition (15) is key, as we can apply first a fast subsampling sketch, and then a sub-Gaussian sketch on the sub-sampled Gram matrix of reduced size. Overall, computing SKS^\top requires at most $\mathcal{O}(ss'^2)$ operations, that is always smaller than $\mathcal{O}(sn^2)$. Regarding space complexity, it only requires $\mathcal{O}(s'^2 + ss')$, as we do not store the full Gram matrix in memory.

In addition to be computational efficient, p -sparsified sketches are K -satisfiable with high probability.

Theorem 6. *Let S be a p -sparsified sketch. Then, there exists some universal constants $C_0, C_1 > 0$ and a constant $c(p)$, increasing with p , such that for $s \geq \max(C_0 d_n/p^2, \delta_n^2 n)$ and with a probability at least $1 - C_1 e^{-sc(p)}$, S is a K -satisfiable sketch matrix.*

Proof sketch. The proof leverages the Bernoulli vision of p -sparsified sketches, i.e., that we have $S_{ij} = (1/\sqrt{sp})B_{ij}R_{ij}$ with B_{ij} Bernoulli random variables and R_{ij} sub-Gaussian variables. To prove the l.h.s. of (4), we then use [13, Theorem 2.13], that shows that any sketch matrix with i.i.d. sub-Gaussian entries satisfies the Johnson-Lindenstrauss lemma with high probability. To prove the r.h.s. of (4), we work conditionally on a realization of the Bernoulli matrix, and use standard concentration results of Lipschitz functions of Rademacher or Gaussian random variables [69]. \square

The role of p is pretty intuitive: when p decreases, s' and $c(p)$ decrease too. This means that computations become faster, at the cost of degraded theoretical guarantees though. Identifying an optimal value for p is a highly nontrivial question, that crucially depends on the computational efficiency or statistical accuracy targeted by the learner on a specific problem. We nonetheless highlight that the tradeoffs achieved by p -sparsified sketches for different values of s and p are generally more interesting than that attained by previous approaches, see Figure 1(c). Note that an important line of research is devoted to improve the statistical performance of the (fast but inaccurate) Nyström approximation, either by considering adaptive sampling [41, 71, 31], or sampling based on leverage scores [3, 55, 58, 21]. We somehow take the opposite route, as p -SG sketches can be seen as an accelerated but statistically degraded version of standard Gaussian sketches.

¹Precisely, S_{SS} is the identity matrix $I_{s'}$, augmented with $n - s'$ null columns inserted at the indices of the null columns of S , see Appendix C for more details.

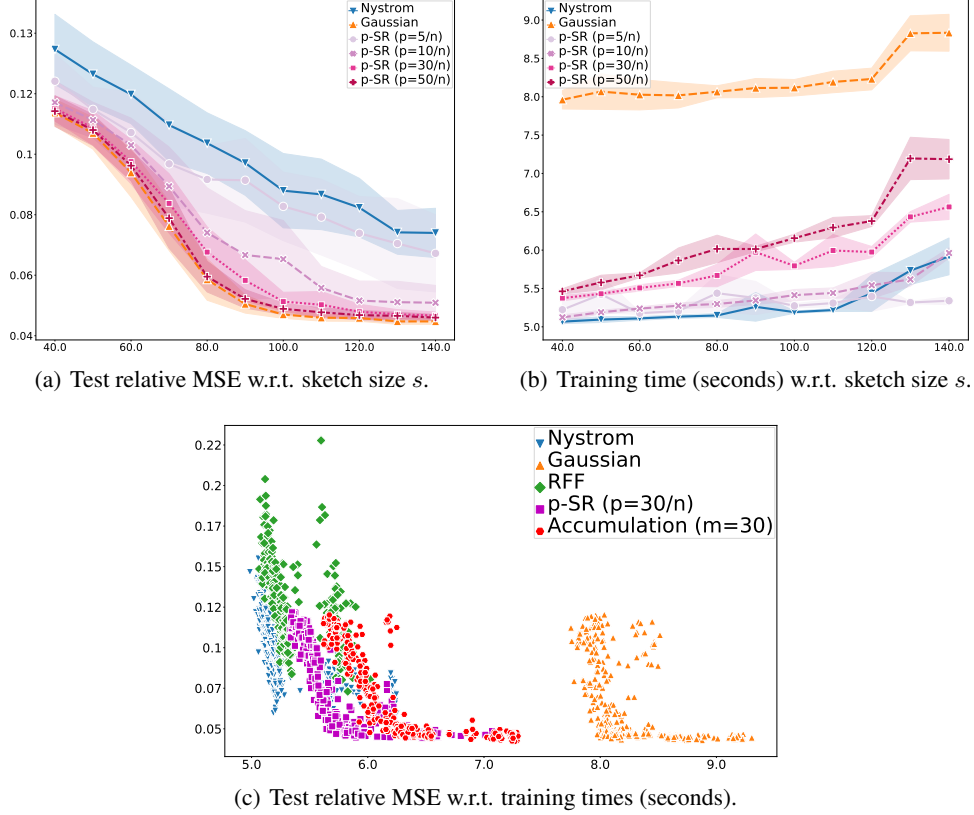


Figure 1: Trade-off between Accuracy and Efficiency for p -SR sketches with κ -Huber loss.

4 Experiments

We now empirically compare the performance of p -sparsified sketches against SOTA approaches.

Scalar regression. We generate a dataset composed of 10,000 datapoints: 9,900 input points are drawn i.i.d. from $\mathcal{U}([0_{10}, 1_{10}])$ and the other 100 input points are drawn i.i.d. from $\mathcal{N}(1.5\mathbb{1}_{10}, 0.25I_{10})$. All the outputs are generated as $y = f^*(x) + \epsilon$, where $\epsilon \sim \mathcal{N}(0, 1)$ and

$$f^*(x) = 0.1 \exp(4x_1) + \frac{4}{1 + \exp(-20(x_2 - 0.5))} + 3x_3 + 2x_4 + x_5,$$

as introduced in [29]. We used the Gaussian kernel and selected its bandwidth—as well as parameters κ (and ϵ for ϵ -SVR)—via 5-folds cross-validation. We solve this 1D regression problem using the κ -Huber loss, described in Appendix F. We learn the sketched kernel machines for different values of s (from 40 to 140) and several values of p , the probability of being non-null in a p -SR sketch. Figure 1(a) presents the test error as a function of the sketch size s . Figure 1(b) shows the corresponding computational training time. All methods reduce their test error, measured in terms of the relative Mean Squared Error (MSE) when s increases. Note that increasing p increases both the precision and the training time, as expected. This behaviour recalls the Accumulation sketches from [20], since we observe a form of interpolation between the Nyström and Gaussian approximations. The behaviour of all the different sketched kernel machines is shown in Figure 1(c), where each of them appears as a point (training time, test MSE). We observe that p -SR sketches attain the smallest possible error ($MSE \leq 0.05$) at a lowest training time budget (mostly around $5.6 < \text{time} < 6.6$). Moreover, p -SR sketches obtain a similar precision range as the Accumulation sketches, but for smaller training times (both approaches improve upon the Gaussian sketch in that respect). Nyström sketching is faster to compute but does not reach the same small test errors like the other schemes. The same phenomenon occurs for Random Fourier Features. This might be explained by the fact that the features are non data-dependent, which make them faster to compute but less performing in this case. We defer to Appendix G.1 similar analyses with p -SG sketches and in ϵ -SVR framework.

Table 1: Empirical test pinball and crossing and training times (in s) obtained without Sketching and with Sketching of size $s = 100$ for Boston dataset and $s = 200$ for Otoliths dataset.

Dataset	Metrics	w/o Sketch	$20/n_{tr}$ -SR	$20/n_{tr}$ -SG	Acc. $m = 20$
Boston	Pinball loss	51.00 \pm 0.81	53.63 \pm 0.72	53.65 \pm 0.67	53.59 \pm 0.75
	Crossing loss	0.42 \pm 0.13	0.31 \pm 0.10	0.21 \pm 0.08	0.30 \pm 0.10
	Training time	5.8 \pm 0.1	1.8 \pm 0.1	1.9 \pm 0.1	2.2 \pm 0.1
otoliths	Pinball loss	2.78	2.54 \pm 0.01	2.55 \pm 0.01	2.53 \pm 0.01
	Crossing loss	5.18	5.36 \pm 0.04	5.38 \pm 0.05	5.36 \pm 0.05
	Training time	408	53 \pm 1.5	51 \pm 0.9	54 \pm 0.2

Table 2: ARRME and training times (in s) with square loss and $s = 200$ when using Sketching.

Dataset	Metrics	w/o Sketch	$20/n_{tr}$ -SR	$20/n_{tr}$ -SG	Acc. $m = 20$
rf1	ARRMSE	0.575	0.582 \pm 0.002	0.583 \pm 0.002	0.575 \pm 0.0002
	Training time	1.81	0.45 \pm 0.009	0.48 \pm 0.026	1.31 \pm 0.073
rf2	ARRMSE	0.578	0.629 \pm 0.003	0.628 \pm 0.002	0.627 \pm 0.003
	Training time	1.37	0.55 \pm 0.015	0.59 \pm 0.015	1.75 \pm 0.015
scm1d	ARRMSE	0.419	0.418 \pm 0.0002	0.419 \pm 0.0001	0.420 \pm 0.0003
	Training time	5.72	0.86 \pm 0.034	0.90 \pm 0.031	2.07 \pm 0.037
scm20d	ARRMSE	0.751	0.753 \pm 0.001	0.752 \pm 0.001	0.752 \pm 0.001
	Training time	7.30	0.71 \pm 0.02	0.72 \pm 0.01	1.89 \pm 0.05

Vector-valued regression. *Joint quantile regression* [60]. We chose the quantile levels as follows $\tau = (0.1, 0.3, 0.5, 0.7, 0.9)$. We apply a subgradient algorithm to minimize the pinball loss described in Appendix F with ridge regularization and a kernel $\mathcal{K} = kM$ with M discussed in Example 1, and k a Gaussian kernel. We showcase the behaviour of the proposed algorithm for Joint Sketched Quantile Regression on two datasets: the Boston Housing dataset [33], composed of 506 data points devoted to house price prediction, and the Fish Otoliths dataset [54, 56], dedicated to fish age prediction from images of otoliths (calcium carbonate structures), composed of a train and test sets of size 3780 and 165 respectively. The results are averages over 10 random 70% – 30% train-test splits for Boston dataset. For the Otoliths dataset we kept the initial given train-test split, and for each sketch type, averaged over 30 replicates. The results are reported in Table 1. Sketching allows for a massive reduction of the training times while preserving the statistical performances. As a comparison, according to the results stated in [60], the best benchmark result for the Boston dataset in terms of test pinball loss is 47.4, while best test crossing loss is 0.48, which shows that our implementation does not compete in terms of quantile prediction but preserves the non-crossing property.

Multi-output regression [63]. We finally conducted experiments on multi-output kernel ridge regression. We used decomposable kernels, and took the largest datasets² introduced in [63]. They consist in four datasets, divided in two groups: River Flow (rf1 and rf2) both composed of 4108 training data, and Supply Chain Management (scm1d and scm20d) composed of 8145 and 7463 training data respectively (more details and additional results can be found in Appendix G.2). We compare our non-sketched decomposable matrix-valued kernel machine with the sketched version. For the sake of conciseness, we only report here the Average Relative Root Mean Squared Error (ARRMSE) over all targets (Table 2, see Appendix G.2 for the rest). For all datasets, sketching shows strong computational improvements while maintaining an accuracy of the same order as without sketching. Note however that kernel methods on these problems achieve performance in the range of SOTA methods, but do not reach the best performance (see Appendix G.2 for more details).

Note that for both joint quantile regression and multi-output regression the results obtained after sketching (no matter the sketch chosen) are almost the same as that attained without sketching. It might be explained by two factors. First, the datasets studied have relatively small training sizes (from 354 training data for Boston to 8145 for scm1d). Second, predicting jointly multiple outputs is a complex task, so that it appears more natural to obtain less differences and variance using various types of sketches (or no sketch). However, in all cases sketching induces a huge time saver.

²available at <http://mulan.sourceforge.net/datasets-mtr.html>.

Acknowledgements

The authors thank Olivier Fercoq for insightful discussions. This work was supported by the Télécom Paris research chair on Data Science and Artificial Intelligence for Digitalized Industry and Services (DSADIS).

References

- [1] Dimitris Achlioptas. Database-friendly random projections. In *Proceedings of the twentieth ACM SIGMOD-SIGACT-SIGART symposium on Principles of database systems*, pages 274–281, 2001.
- [2] Ahmet Alacaoglu, Olivier Fercoq, and Volkan Cevher. Random extrapolation for primal-dual coordinate descent. In *Proc of the International Conference on Machine Learning (ICML)*, pages 191–201. PMLR, 2020.
- [3] Ahmed Alaoui and Michael W Mahoney. Fast randomized kernel ridge regression with statistical guarantees. In C. Cortes, N. Lawrence, D. Lee, M. Sugiyama, and R. Garnett, editors, *Advances in Neural Information Processing Systems (NeurIPS)*, volume 28, 2015.
- [4] Mauricio A. Álvarez, Lorenzo Rosasco, and Neil D. Lawrence. Kernels for vector-valued functions: a review. *Foundations and Trends in Machine Learning*, 4(3):195–266, 2012.
- [5] Nachman Aronszajn. Theory of reproducing kernels. *Transactions of the American Mathematical Society*, pages 337–404, 1950.
- [6] Haim Avron, Kenneth L Clarkson, and David P Woodruff. Faster kernel ridge regression using sketching and preconditioning. *SIAM Journal on Matrix Analysis and Applications*, 38(4):1116–1138, 2017.
- [7] Francis Bach. Sharp analysis of low-rank kernel matrix approximations. In *Proc. of the 26th annual Conference on Learning Theory*, pages 185–209. PMLR, 2013.
- [8] Luca Baldassarre, Lorenzo Rosasco, Annalisa Barla, and Alessandro Verri. Multi-output learning via spectral filtering. *Machine Learning*, 87(3):259–301, 2012.
- [9] Richard Baraniuk, Mark Davenport, Ronald DeVore, and Michael Wakin. A simple proof of the restricted isometry property for random matrices. *Constructive Approximation*, 28(3):253–263, 2008.
- [10] Peter L. Bartlett, Olivier Bousquet, and Shahar Mendelson. Local rademacher complexities. *Ann. Statist.*, 33(4):1497–1537, 2005.
- [11] Peter L Bartlett, Michael I Jordan, and Jon D McAuliffe. Convexity, classification, and risk bounds. *Journal of the American Statistical Association*, 101(473):138–156, 2006.
- [12] Peter L. Bartlett and Shahar Mendelson. Rademacher and gaussian complexities: Risk bounds and structural results. *J. Mach. Learn. Res.*, 3:463–482, 2003.
- [13] Stéphane Boucheron, Gábor Lugosi, and Pascal Massart. *Concentration inequalities: A nonasymptotic theory of independence*. Oxford university press, 2013.
- [14] Romain Brault, Markus Heinonen, and Florence Buc. Random fourier features for operator-valued kernels. In *Asian Conference on Machine Learning*, pages 110–125. PMLR, 2016.
- [15] Andrea Caponnetto and Ernesto De Vito. Optimal rates for the regularized least-squares algorithm. *Foundations of Computational Mathematics*, 7(3):331–368, 2007.
- [16] Claudio Carmeli, Ernesto De Vito, and Alessandro Toigo. Vector valued reproducing kernel hilbert spaces of integrable functions and mercer theorem. *Analysis and Applications*, 4(04):377–408, 2006.

- [17] Claudio Carmeli, Ernesto De Vito, Alessandro Toigo, and Veronica Umanitá. Vector valued reproducing kernel hilbert spaces and universality. *Analysis and Applications*, 8(01):19–61, 2010.
- [18] Antonin Chambolle, Matthias J Ehrhardt, Peter Richtárik, and Carola-Bibiane Schonlieb. Stochastic primal-dual hybrid gradient algorithm with arbitrary sampling and imaging applications. *SIAM Journal on Optimization*, 28(4):2783–2808, 2018.
- [19] Antoine Chatalic, Luigi Carratino, Ernesto De Vito, and Lorenzo Rosasco. Mean nystrom embeddings for adaptive compressive learning, 2021.
- [20] Yifan Chen and Yun Yang. Accumulations of projections—a unified framework for random sketches in kernel ridge regression. In *International Conference on Artificial Intelligence and Statistics*, pages 2953–2961. PMLR, 2021.
- [21] Yifan Chen and Yun Yang. Fast statistical leverage score approximation in kernel ridge regression. In *International Conference on Artificial Intelligence and Statistics*, pages 2935–2943. PMLR, 2021.
- [22] Laurent Condat. A primal–dual splitting method for convex optimization involving lipschitzian, proximable and linear composite terms. *Journal of optimization theory and applications*, 158(2):460–479, 2013.
- [23] Corinna Cortes and Vladimir Vapnik. Support-vector networks. *Machine learning*, 20(3):273–297, 1995.
- [24] Andrea Della Vecchia, Jaouad Mourtada, Ernesto De Vito, and Lorenzo Rosasco. Regularized erm on random subspaces. In *International Conference on Artificial Intelligence and Statistics*, pages 4006–4014. PMLR, 2021.
- [25] Petros Drineas, Michael W Mahoney, and Nello Cristianini. On the nystrom method for approximating a gram matrix for improved kernel-based learning. *JMLR*, 6(12), 2005.
- [26] Harris Drucker, Christopher JC Burges, Linda Kaufman, Alex J Smola, and Vladimir Vapnik. Support vector regression machines. In *Advances in neural information processing systems*, pages 155–161, 1997.
- [27] Theodoros Evgeniou, Charles A. Micchelli, and Massimiliano Pontil. Learning multiple tasks with kernel methods. *Journal of Machine Learning Research*, 6(21):615–637, 2005.
- [28] Olivier Fercoq and Pascal Bianchi. A coordinate-descent primal-dual algorithm with large step size and possibly nonseparable functions. *SIAM Journal on Optimization*, 29(1):100–134, Jan 2019.
- [29] Jerome H Friedman. Multivariate adaptive regression splines. *The annals of statistics*, pages 1–67, 1991.
- [30] Nidham Gazagnadou, Mark Ibrahim, and Robert M. Gower. RidgeSketch: A fast sketching based solver for large scale ridge regression, 2021.
- [31] Alex Gittens and Michael Mahoney. Revisiting the nystrom method for improved large-scale machine learning. *Proceedings of the 30th International Conference on Machine Learning*, 28(3):567–575, 17–19 Jun 2013.
- [32] William Groves and Maria Gini. On optimizing airline ticket purchase timing. *ACM Transactions on Intelligent Systems and Technology (TIST)*, 7(1):1–28, 2015.
- [33] David Harrison Jr and Daniel L Rubinfeld. Hedonic housing prices and the demand for clean air. *Journal of environmental economics and management*, 5(1):81–102, 1978.
- [34] Matthias Hein and Olivier Bousquet. Kernels, associated structures and generalizations. Technical Report 127, Max Planck Institute for Biological Cybernetics, Tübingen, Germany, July 2004.

- [35] Peter J Huber. Robust estimation of a location parameter. *The Annals of Mathematical Statistics*, pages 73–101, 1964.
- [36] William B Johnson and Joram Lindenstrauss. Extensions of lipschitz mappings into a hilbert space 26. *Contemporary mathematics*, 26:28, 1984.
- [37] George Kimeldorf and Grace Wahba. Some results on tchebycheffian spline functions. *Journal of mathematical analysis and applications*, 33(1):82–95, 1971.
- [38] Diederik P. Kingma and Jimmy Ba. Adam: A method for stochastic optimization. In Yoshua Bengio and Yann LeCun, editors, *3rd International Conference on Learning Representations, ICLR 2015, San Diego, CA, USA, May 7-9, 2015, Conference Track Proceedings*, 2015.
- [39] Roger Koenker. *Quantile regression*. Cambridge university press, 2005.
- [40] Samory Kpotufe and Bharath K. Sriperumbudur. Gaussian sketching yields a J-L lemma in RKHS. In Silvia Chiappa and Roberto Calandra, editors, *AISTATS 2020*, volume 108 of *Proceedings of Machine Learning Research*, pages 3928–3937. PMLR, 2020.
- [41] Sanjiv Kumar, Mehryar Mohri, and Ameet Talwalkar. Sampling methods for the nyström method. *J. Mach. Learn. Res.*, 13:981–1006, 2012.
- [42] Jonathan Lacotte and Mert Pilanci. Adaptive and oblivious randomized subspace methods for high-dimensional optimization: Sharp analysis and lower bounds. *arXiv preprint arXiv:2012.07054*, 2020.
- [43] Jonathan Lacotte, Mert Pilanci, and Marco Pavone. High-dimensional optimization in adaptive random subspaces. In *Proc. of the 33rd International Conference on Neural Information Processing Systems*, pages 10847–10857, 2019.
- [44] Pierre Laforgue, Alex Lambert, Luc Brogat-Motte, and Florence d’Alché Buc. Duality in rkhs with infinite dimensional outputs: Application to robust losses. In *International Conference on Machine Learning*, pages 5598–5607. PMLR, 2020.
- [45] Ping Li, Trevor J Hastie, and Kenneth W Church. Very sparse random projections. In *Proceedings of the 12th ACM SIGKDD international conference on Knowledge discovery and data mining*, pages 287–296, 2006.
- [46] Zhe Li, Tianbao Yang, Lijun Zhang, and Rong Jin. Fast and accurate refined nyström-based kernel svm. In *Thirtieth AAAI Conference on Artificial Intelligence*, 2016.
- [47] Zhu Li, Jean-Francois Ton, Dino Oglic, and Dino Sejdinovic. Towards a unified analysis of random fourier features. *Journal of Machine Learning Research*, 22(108):1–51, 2021.
- [48] Meimei Liu, Zuofeng Shang, and Guang Cheng. Sharp theoretical analysis for nonparametric testing under random projection. In Alina Beygelzimer and Daniel Hsu, editors, *Proceedings of the Thirty-Second Conference on Learning Theory*, volume 99 of *Proceedings of Machine Learning Research*, pages 2175–2209. PMLR, 25–28 Jun 2019.
- [49] Michael W Mahoney et al. Randomized algorithms for matrices and data. *Foundations and Trends® in Machine Learning*, 3(2):123–224, 2011.
- [50] Jiří Matoušek. *Lectures on Discrete Geometry*. Graduate Texts in Mathematics. Springer, 2013.
- [51] Andreas Maurer. A vector-contraction inequality for rademacher complexities. In *International Conference on Algorithmic Learning Theory*, pages 3–17. Springer, 2016.
- [52] Giacomo Meanti, Luigi Carratino, Lorenzo Rosasco, and Alessandro Rudi. Kernel methods through the roof: Handling billions of points efficiently. *Advances in Neural Information Processing Systems (NeurIPS)*, 33, 2020.
- [53] Charles A Micchelli and Massimiliano Pontil. On learning vector-valued functions. *Neural computation*, 17(1):177–204, 2005.

- [54] Endre Moen, Nils Olav Handegard, Vaneeda Allken, Ole Thomas Albert, Alf Harbitz, and Ketil Malde. Automatic interpretation of otoliths using deep learning. *PLoS One*, 13(12):e0204713, 2018.
- [55] Cameron Musco and Christopher Musco. Recursive sampling for the nyström method. *Advances in Neural Information Processing Systems*, 2017:3834–3846, 2017.
- [56] Alba Ordoñez, Line Eikvil, Arnt-Børre Salberg, Alf Harbitz, Sean Meling Murray, and Michael C Kampffmeyer. Explaining decisions of deep neural networks used for fish age prediction. *PloS one*, 15(6):e0235013, 2020.
- [57] Ali Rahimi and B. Recht. Random features for large scale kernel machines. *NIPS*, 20:1177–1184, 01 2007.
- [58] Alessandro Rudi, Daniele Calandriello, Luigi Carratino, and Lorenzo Rosasco. On fast leverage score sampling and optimal learning. In *NeurIPS*, 2018.
- [59] Alessandro Rudi and Lorenzo Rosasco. Generalization properties of learning with random features. In *Advances on Neural Information Processing Systems (NeurIPS)*, pages 3215–3225, 2017.
- [60] Maxime Sangnier, Olivier Fercoq, and Florence d’Alché Buc. Joint quantile regression in vector-valued RKHSs. In *Advances in Neural Information Processing Systems (NeurIPS)*, Barcelona, France, December 2016.
- [61] Bernhard Scholkopf and Alexander J Smola. *Learning with kernels: support vector machines, regularization, optimization, and beyond*. Adaptive Computation and Machine Learning Series, 2018.
- [62] Daniel Sheldon. Graphical multi-task learning, 2008.
- [63] Eleftherios Spyromitros-Xioufis, Grigorios Tsoumakas, William Groves, and Ioannis Vlahavas. Multi-target regression via input space expansion: treating targets as inputs. *Machine Learning*, 104(1):55–98, 2016.
- [64] Bharath K Sriperumbudur and Zoltán Szabó. Optimal rates for random fourier features. In *NIPS*, 2015.
- [65] Ingo Steinwart and Andreas Christmann. Sparsity of svms that use the epsilon-insensitive loss. In Daphne Koller, Dale Schuurmans, Yoshua Bengio, and Léon Bottou, editors, *Advances in Neural Information Processing Systems 21 (NeurIPS)*, pages 1569–1576. Curran Associates, Inc., 2008.
- [66] Ingo Steinwart and Andreas Christmann. *Support vector machines*. Springer Science & Business Media, 2008.
- [67] Ingo Steinwart and Andreas Christmann. Estimating conditional quantiles with the help of the pinball loss. *Bernoulli*, 17(1):211–225, 2011.
- [68] Michel Talagrand. Concentration of measure and isoperimetric inequalities in product spaces. *Publications Mathématiques de l’Institut des Hautes Etudes Scientifiques*, 81(1):73–205, 1995.
- [69] Terence Tao. *Topics in random matrix theory*, volume 132. American Mathematical Soc., 2012.
- [70] Bang Cong Vu. A splitting algorithm for dual monotone inclusions involving cocoercive operators, 2011.
- [71] Shusen Wang and Zhihua Zhang. Improving cur matrix decomposition and the nyström approximation via adaptive sampling. *J. Mach. Learn. Res.*, 14(1):2729–2769, jan 2013.
- [72] Christopher Williams and Matthias Seeger. Using the nyström method to speed up kernel machines. In T. Leen, T. Dietterich, and V. Tresp, editors, *Advances in Neural Information Processing Systems*, volume 13, pages 682–688. MIT Press, 2001.

- [73] David P. Woodruff. Sketching as a tool for numerical linear algebra. *Found. Trends Theor. Comput. Sci.*, 10(1-2):1–157, 2014.
- [74] Tianbao Yang, Yu-feng Li, Mehrdad Mahdavi, Rong Jin, and Zhi-Hua Zhou. Nyström method vs random fourier features: A theoretical and empirical comparison. In F. Pereira, C. J. C. Burges, L. Bottou, and K. Q. Weinberger, editors, *Advances in Neural Information Processing Systems*, volume 25. Curran Associates, Inc., 2012.
- [75] Yun Yang, Mert Pilanci, Martin J Wainwright, et al. Randomized sketches for kernels: Fast and optimal nonparametric regression. *The Annals of Statistics*, 45(3):991–1023, 2017.
- [76] Kai Zhang, Liang Lan, Zhuang Wang, and Fabian Moerchen. Scaling up kernel svm on limited resources: A low-rank linearization approach. In Neil D. Lawrence and Mark Girolami, editors, *Proceedings of the Fifteenth International Conference on Artificial Intelligence and Statistics*, volume 22, pages 1425–1434, 2012.

A Technical Proofs

In this section are gathered all the technical proofs of the results stated in the article.

Notation. We recall that we assume that training data $(x_i, y_i)_{i=1}^n$ are i.i.d. realisations sampled from a joint probability density $P(x, y)$. We define

$$\begin{aligned}\mathbb{E}_n[\ell_f] &= \frac{1}{n} \sum_{i=1}^n \ell(f(x_i), y_i), \\ \mathbb{E}[\ell_f] &= \mathbb{E}_P[\ell(f(X), Y)].\end{aligned}$$

For a class of functions F , the empirical Rademacher complexity [12] is defined as

$$\hat{R}_n(F) = \mathbb{E} \left[\sup_{f \in F} \left| \frac{2}{n} \sum_{i=1}^n \sigma_i f(x_i) \right| \middle| x_1, \dots, x_n \right],$$

where $\sigma_1, \dots, \sigma_n$ are independent Rademacher random variables such that $\mathbb{P}\{\sigma_i = 1\} = \mathbb{P}\{\sigma_i = -1\} = 1/2$. The corresponding Rademacher complexity is then defined as the expectation of the empirical Rademacher complexity

$$R_n(F) = \mathbb{E} [\hat{R}_n(F)].$$

A.1 Proof of Theorem 2

We first prove Equation (5).

Proof. The proof follows the path of the proof of Theorem 3 from [47]. We decompose the expected learning risk as

$$\mathbb{E}[\ell_{\tilde{f}_s}] - \mathbb{E}[\ell_{f_{\mathcal{H}_k}}] = \mathbb{E}[\ell_{\tilde{f}_s}] - \mathbb{E}_n[\ell_{\tilde{f}_s}] + \mathbb{E}_n[\ell_{\tilde{f}_s}] - \mathbb{E}_n[\ell_{f_{\mathcal{H}_k}}] + \mathbb{E}_n[\ell_{f_{\mathcal{H}_k}}] - \mathbb{E}[\ell_{f_{\mathcal{H}_k}}]. \quad (7)$$

Then, we use the following lemma [12, Theorem 8] to bound $\mathbb{E}[\ell_{\tilde{f}_s}] - \mathbb{E}_n[\ell_{\tilde{f}_s}]$ and $\mathbb{E}_n[\ell_{f_{\mathcal{H}_k}}] - \mathbb{E}[\ell_{f_{\mathcal{H}_k}}]$.

Lemma 7. [12, Theorem 8] *Let $\{x_i, y_i\}_{i=1}^n$ be i.i.d samples from P and let \mathcal{H} be the space of functions mapping from \mathcal{X} to \mathbb{R} . Denote a loss function with $l : \mathcal{Y} \times \mathbb{R} \rightarrow [0, 1]$ and recall the learning risk function for all $f \in \mathcal{H}$ is $\mathbb{E}[l_f]$, together with the corresponding empirical risk function $\mathbb{E}_n[l_f] = (1/n) \sum_{i=1}^n l(y_i, f(x_i))$. Then, for a sample of size n , for all $f \in \mathcal{H}$ and $\delta \in (0, 1)$, with probability $1 - \delta$, we have that*

$$\mathbb{E}[l_f] \leq \mathbb{E}_n[l_f] + R_n(l \circ \mathcal{H}) + \sqrt{\frac{8 \log(2/\delta)}{n}}$$

where $l \circ \mathcal{H} = \{(x, y) \rightarrow l(y, f(x)) - l(y, 0) \mid f \in \mathcal{H}\}$.

Thus, since \tilde{f}_s lies in the unit ball $\mathcal{B}(\mathcal{H}_k)$ of \mathcal{H}_k by Assumption 1, we obtain thanks to the above lemma, with a probability at least $1 - \delta$

$$\mathbb{E}[\ell_{\tilde{f}_s}] - \mathbb{E}_n[\ell_{\tilde{f}_s}] \leq R_n(\ell \circ \mathcal{B}(\mathcal{H}_k)) + \sqrt{\frac{8 \log(2/\delta)}{n}}.$$

Then, by the Lipschitz continuity of ℓ (Assumption 2) and point 4 of Theorem 12 from [12], we have that

$$R_n(\ell \circ \mathcal{B}(\mathcal{H}_k)) \leq 2LR_n(\mathcal{B}(\mathcal{H}_k)).$$

Finally, Assumption 3 combined with Lemma 22 from [12] then yields

$$R_n(\mathcal{B}(\mathcal{H}_k)) \leq \frac{2}{n} \sqrt{\sum_{i=1}^n k(x_i, x_i)} \leq 2\sqrt{\frac{\kappa}{n}}.$$

As a consequence, we obtain

$$\mathbb{E}[\ell_{\tilde{f}_s}] - \mathbb{E}_n[\ell_{\tilde{f}_s}] \leq \frac{4L\sqrt{\kappa}}{\sqrt{n}} + \sqrt{\frac{8 \log(2/\delta)}{n}}, \quad (16)$$

and the exact same result applies to $\mathbb{E}_n[\ell_{f_{\mathcal{H}_k}}] - \mathbb{E}[\ell_{f_{\mathcal{H}_k}}]$, by Assumption 1 and the opposite side of Lemma 7.

We now focus on the last quantity to bound. Let $\mathcal{H}_S = \{f = \sum_{i=1}^n [S^\top \gamma]_i k(\cdot, x_i) \mid \gamma \in \mathbb{R}^s\}$. By Assumption 2 and Jensen's inequality we have

$$\begin{aligned} \mathbb{E}_n[\ell_{\tilde{f}_s}] - \mathbb{E}_n[\ell_{f_{\mathcal{H}_k}}] &= \frac{1}{n} \sum_{i=1}^n l(\tilde{f}_s(x_i), y_i) - \frac{1}{n} \sum_{i=1}^n l(f_{\mathcal{H}_k}(x_i), y_i) \\ &= \inf_{\substack{f \in \mathcal{H}_S \\ \|f\|_{\mathcal{H}_k} \leq 1}} \frac{1}{n} \sum_{i=1}^n l(f(x_i), y_i) - \frac{1}{n} \sum_{i=1}^n l(f_{\mathcal{H}_k}(x_i), y_i) \\ &\leq \inf_{\substack{f \in \mathcal{H}_S \\ \|f\|_{\mathcal{H}_k} \leq 1}} \frac{L}{n} \sum_{i=1}^n |f(x_i) - f_{\mathcal{H}_k}(x_i)| \\ &\leq L \inf_{\substack{f \in \mathcal{H}_S \\ \|f\|_{\mathcal{H}_k} \leq 1}} \sqrt{\frac{1}{n} \sum_{i=1}^n |f(x_i) - f_{\mathcal{H}_k}(x_i)|^2} \\ &\leq L \inf_{\substack{f \in \mathcal{H}_S \\ \|f\|_{\mathcal{H}_k} \leq 1}} \sqrt{\frac{1}{n} \|f^X - f_{\mathcal{H}_k}^X\|_2^2}, \end{aligned}$$

where, for any $f \in \mathcal{H}_k$, $f^X = (f(x_1), \dots, f(x_n)) \in \mathbb{R}^n$. Let $\tilde{f}_s^R = \sum_{i=1}^n [S^\top \tilde{\gamma}^R]_i k(\cdot, x_i)$, where $\tilde{\gamma}^R$ is a solution to

$$\inf_{\gamma \in \mathbb{R}^s} \frac{1}{n} \|KS^\top \gamma - f_{\mathcal{H}_k}^X\|_2^2 + \lambda \gamma^\top SKS^\top \gamma.$$

It is easy to check that \tilde{f}_s^R is also a solution to

$$\inf_{\substack{f \in \mathcal{H}_S \\ \|f\|_{\mathcal{H}_k} \leq \|\tilde{f}_s\|_{\mathcal{H}_k}}} \frac{1}{n} \|f^X - f_{\mathcal{H}_k}^X\|_2^2.$$

Since we have $\|\tilde{f}_s^R\|_{\mathcal{H}_k} \leq 1$ by Assumption 1, it holds

$$\begin{aligned} \inf_{\substack{f \in \mathcal{H}_S \\ \|f\|_{\mathcal{H}_k} \leq 1}} \frac{1}{n} \|f^X - f_{\mathcal{H}_k}^X\|_2^2 &\leq \inf_{\substack{f \in \mathcal{H}_S \\ \|f\|_{\mathcal{H}_k} \leq \|\tilde{f}_s\|_{\mathcal{H}_k}}} \frac{1}{n} \|f^X - f_{\mathcal{H}_k}^X\|_2^2 \\ &= \inf_{\gamma \in \mathbb{R}^s} \frac{1}{n} \|KS^\top \gamma - f_{\mathcal{H}_k}^X\|_2^2 + \lambda \gamma^\top SKS^\top \gamma. \end{aligned}$$

As a consequence,

$$\mathbb{E}_n [l_{\tilde{f}_s}] - \mathbb{E}_n [l_{f_{\mathcal{H}_k}}] \leq L \sqrt{\inf_{\gamma \in \mathbb{R}^s} \frac{1}{n} \|KS^\top \gamma - f_{\mathcal{H}_k}^X\|_2^2 + \lambda \gamma^\top SKS^\top \gamma}.$$

Finally, since S is a K -satisfiable sketch matrix, using Lemma 2 from [75],

$$\mathbb{E}_n [l_{\tilde{f}_s}] - \mathbb{E}_n [l_{f_{\mathcal{H}_k}}] \leq LC \sqrt{\lambda + \delta_n^2}, \quad (17)$$

where $C = 1 + \sqrt{6}c$ and c is a universal constant coming from K -satisfiable property. The desired bound is obtained by combining Equations (7), (16) and (17). \square

We now give the proof of the second claim (Equation (6)), i.e., the excess risk bound for kernel ridge regression.

Proof. We now assume that the outputs are bounded, hence, without loss of generality, let assume $\mathcal{Y} \subset [0, 1]$. First, we prove Lipschitz-continuity of the square loss under Assumptions 1 and 3. Let $g : z \in \mathcal{H}_k(\mathcal{X}) \mapsto \frac{1}{2}(z - y)^2$, for $y \in [0, 1]$. Hence, $g'(z) = z - y$ and by Assumptions 1 and 3

$$|g'(z)| \leq |z| + |y| \leq |f(x)| + 1 \leq |\langle f, k(\cdot, x) \rangle_{\mathcal{H}_k}| + 1 \leq \|f\|_{\mathcal{H}_k} \kappa^{1/2} + 1 = \kappa^{1/2} + 1,$$

for some $f \in \mathcal{H}_k$ and $x \in \mathcal{X}$ since $z \in \mathcal{H}_k(\mathcal{X})$. As a consequence, we obtain that g is $(\kappa^{1/2} + 1)$ -Lipschitz, i.e.

$$|\ell(f(x), y) - \ell(f'(x'), y)| \leq (\kappa^{1/2} + 1) |f(x) - f'(x')|.$$

We can then obtain the same generalisation bounds as above. Finally, looking at the approximation term,

$$\begin{aligned} \mathbb{E}_n [l_{\tilde{f}_s}] - \mathbb{E}_n [l_{f_{\mathcal{H}_k}}] &= \frac{1}{2n} \|\tilde{f}_s^X - Y\|_2^2 - \frac{1}{2n} \|f_{\mathcal{H}_k}^X - Y\|_2^2 \\ &\leq \frac{1}{2n} \|\tilde{f}_s^X - f_{\mathcal{H}_k}^X\|_2^2 \\ &\leq \inf_{\substack{f \in \mathcal{H}_S \\ \|f\|_{\mathcal{H}_k} \leq 1}} \frac{1}{2n} \|f^X - f_{\mathcal{H}_k}^X\|_2^2 \\ &\leq \inf_{\gamma \in \mathbb{R}^s} \frac{1}{n} \|KS^\top \gamma - f_{\mathcal{H}_k}^X\|_2^2 + \lambda \gamma^\top SKS^\top \gamma \\ &\leq C^2 (\lambda + \delta_n^2). \end{aligned}$$

We obtain the same bound as above without the square root since we do not need to invoke Jensen inequality as the studied loss is the square loss. Gathering all arguments, we obtain Equation (6). \square

A.2 Refined analysis in the scalar case

As said in Remark 1, and similarly to [47], we can conduct a refined analysis, leading to faster convergence rates for the generalization errors, with the following additional assumption.

Assumption 5. *There is a constant B such that, for all $f \in \mathcal{H}_k$ we have*

$$\mathbb{E} [f - f_{\mathcal{H}_k}]^2 \leq B \mathbb{E} [l_f - l_{f_{\mathcal{H}_k}}]. \quad (18)$$

It has been shown that many loss functions satisfy this assumption such as Hinge loss [66, 11], truncated quadratic or sigmoid loss [11]. Under Assumptions 1 to 4 and 5, the following result holds:

Theorem 8. *We define, for $\delta \in (0, 1)$, the following sub-root function $\hat{\psi}_n$*

$$\hat{\psi}_n(r) = 2LC_1 \left(\frac{2}{n} \sum_{i=1}^n \min \{b_2 r, \lambda_i\} \right)^{1/2} + \frac{C_2}{n} \log \frac{1}{\delta},$$

and let $\hat{r}_{\mathcal{H}_k}^*$ be the fixed point of $\hat{\psi}_n$, i.e., $\hat{\psi}_n(\hat{r}_{\mathcal{H}_k}^*) = \hat{r}_{\mathcal{H}_k}^*$. Then, we have for all $D > 1$ and $\delta \in (0, 1)$ with probability greater than $1 - \delta$,

$$\mathbb{E}[\ell_{\tilde{f}_s}] \leq \mathbb{E}[\ell_{f_{\mathcal{H}_k}}] + \frac{D}{D-1} LC \sqrt{\lambda + \delta_n^2} + \frac{12D}{B} \hat{r}_{\mathcal{H}_k}^* + \frac{2C_3}{n} \log \frac{1}{\delta}, \quad (19)$$

where C is as in Theorem 2 and C_1, C_2, C_3 and b_2 are some constants and $\hat{r}_{\mathcal{H}_k}^*$ can be upper bounded by

$$\hat{r}_{\mathcal{H}_k}^* \leq \min_{0 \leq h \leq n} \left(b_0 \frac{h}{n} + \sqrt{\frac{1}{n} \sum_{i>h} \lambda_i} \right),$$

where B and b_0 are some constants.

Hence, we see that, in order to obtain faster learning rates than Theorem 2 as [47], we need to replace δ_n^2 by $\hat{r}_{\mathcal{H}_k}^{*2}$. However, according to the expression of $\hat{\psi}_n$ and its dependencies to non-explicit constants, it appears very difficult to prove that $\left(\frac{1}{n} \sum_{i=1}^n \min(\hat{r}_{\mathcal{H}_k}^{*2}, \lambda_i) \right)^{1/2} \leq \hat{r}_{\mathcal{H}_k}^{*2}$, which is a necessary condition to prove that a sketch matrix S is K -satisfiable. We still prove the above result following the proof of Theorem 4 in [47], and leave as an open problem to find faster rates than δ_n .

Proof. We use the decomposition of the expected learning risk from [47]

$$\begin{aligned} \mathbb{E}[\ell_{\tilde{f}_s}] - \mathbb{E}[\ell_{f_{\mathcal{H}_k}}] &= \mathbb{E}[\ell_{\tilde{f}_s}] - \frac{D}{D-1} \mathbb{E}_n[\ell_{\tilde{f}_s}] \\ &\quad + \frac{D}{D-1} \left(\mathbb{E}_n[\ell_{\tilde{f}_s}] - \mathbb{E}_n[\ell_{f_{\mathcal{H}_k}}] \right) \\ &\quad + \frac{D}{D-1} \mathbb{E}_n[\ell_{f_{\mathcal{H}_k}}] - \mathbb{E}[\ell_{f_{\mathcal{H}_k}}], \end{aligned}$$

for $D > 1$. The generalization errors can be bounded as in [47] by Theorem 8. The approximation error is bounded using (17). \square

A.3 Proof of Theorem 4

Here, the proof uses the same decomposition of the excess risk (Equation (7)) as in single output settings. Since some works [51] exist to easily extend generalisation bounds of functions in scalar-valued RKHS to functions in vector-valued RKHS, the main challenge here is to derive an approximation error for the multiple output settings. Hence, let us first state a needed intermediate results that we will prove later.

Lemma 9. For all $f \in \mathcal{H}_{\mathcal{K}}$, such that $\|f\|_{\mathcal{H}_{\mathcal{K}}} \leq 1$, we have $z^\top (K^{-1} \otimes M^{-1}) z \leq 1$, where $z = (f(x_1)^\top, \dots, f(x_n)^\top)^\top \in \mathbb{R}^{nd}$.

We are now equipped to state the main result that generalises Lemma 2 from [75].

Lemma 10. Let $Z^* = (f^*(x_1), \dots, f^*(x_n))^\top \in \mathbb{R}^{n \times d}$ for any $f^* \in \mathcal{H}_{\mathcal{K}}$ such that $\|f^*\|_{\mathcal{H}_{\mathcal{K}}} \leq 1$, where $\mathcal{K} = kM$, and $S \in \mathbb{R}^{s \times n}$ a K -satisfiable matrix. Then we have

$$\inf_{\Gamma \in \mathbb{R}^{s \times d}} \frac{1}{n} \|KS^\top \Gamma M - Z^*\|_F^2 + \lambda \text{Tr}(KS^\top \Gamma M \Gamma^\top S) \leq C^2 (\|M\|_{\text{op}} \delta_n^2 + \lambda), \quad (20)$$

where $C = 1 + \sqrt{6}c$ and c is the universal constant from Definition 2.

Proof. We adapt the proof of Lemma 2 from [75] to the multidimensional case. If we are able to find a $\Gamma \in \mathbb{R}^{s \times d}$ such that

$$\frac{1}{n} \|KS^\top \Gamma M - Z^*\|_F^2 + \lambda \text{Tr}(KS^\top \Gamma M \Gamma^\top S) \leq C^2 (\|M\|_{\text{op}} \delta_n^2 + \lambda),$$

then in particular it also holds true for the minimizer. We recall the eigendecompositions $\frac{1}{n} K = K_{\text{norm}} = UDU^\top$ and $M = V\Delta V^\top$. Then the above problem rewrites as

$$\|D\tilde{S}^\top \Gamma V \Delta - \Theta^*\|_F^2 + \lambda \text{Tr}(\tilde{S} \tilde{S}^\top \Gamma M \Gamma) \leq C^2 (\|M\|_{\text{op}} \delta_n^2 + \lambda),$$

where $\tilde{S} = SU$ and $\Theta^* = \frac{1}{n^{1/2}} U^\top Z^* V$. We can rewrite $\theta^* = (\Theta_{1:}^*, \dots, \Theta_{n:}^*)^\top = \frac{1}{n^{1/2}} (U^\top \otimes V^\top) z^* \in \mathbb{R}^{nd}$, hence $\|(D^{-1/2} \otimes \Delta^{-1/2}) \theta^*\|_2^2 = z^{*\top} (K^{-1} \otimes M^{-1}) z^*$, with $z^* = (Z_{1:}^*, \dots, Z_{n:}^*)^\top = (f^*(x_1)^\top, \dots, f^*(x_n)^\top)^\top \in \mathbb{R}^{nd}$. By Lemma 9, we have that $\|(D^{-1/2} \otimes \Delta^{-1/2}) \theta^*\|_2 \leq 1$, and using the notation $\gamma = (\Gamma_{1:}, \dots, \Gamma_{s:})^\top \in \mathbb{R}^{sd}$, we can rewrite the above problem as finding a γ such that

$$\|\theta^* - (D\tilde{S}^\top \otimes \Delta V^\top) \gamma\|_2^2 + \lambda \gamma^\top (\tilde{S} D \tilde{S}^\top \otimes M) \gamma \leq C^2 (\|M\|_{\text{op}} \delta_n^2 + \lambda).$$

As in [75], we partition vector $\theta^* \in \mathbb{R}^{nd}$ into two sub-vectors, namely $\theta_1^* \in \mathbb{R}^{d_n d}$ and $\theta_2^* \in \mathbb{R}^{(n-d_n)d}$, the diagonal matrix D into two blocks $D_1 \in \mathbb{R}^{d_n \times d_n}$ and $D_2 \in \mathbb{R}^{(n-d_n) \times (n-d_n)}$ and finally, under the condition $s > d_n$, we let $\tilde{S}_1 \in \mathbb{R}^{s \times d_n}$ and $\tilde{S}_2 \in \mathbb{R}^{s \times (n-d_n)}$ denote the left and right block of \tilde{S} respectively. By the K -satisfiability of S we have

$$\|\tilde{S}_1^\top \tilde{S}_1 - I_{d_n}\|_{\text{op}} \leq \frac{1}{2} \quad \text{and} \quad \|\tilde{S}_2 D_2^{1/2}\|_{\text{op}} \leq c \delta_n^2. \quad (21)$$

By the first inequality, we have that $\tilde{S}_1^\top \tilde{S}_1$ is invertible. In fact, assuming that there exists $x \in \mathbb{R}^{d_n}$ such that $\|x\|_2 = 1$ and $\tilde{S}_1^\top \tilde{S}_1 x = 0$, then $\|(\tilde{S}_1^\top \tilde{S}_1 - I_{d_n})x\| = 1 > \frac{1}{2}$. Then, we can define

$$\hat{\gamma} = \left(\tilde{S}_1 (\tilde{S}_1^\top \tilde{S}_1)^{-1} D_1^{-1} \otimes V \Delta^{-1} \right) \theta_1^*. \quad (22)$$

Hence,

$$\|\theta^* - (D\tilde{S}^\top \otimes \Delta V^\top) \hat{\gamma}\|_2^2 = \|\theta_1^* - (D_1 \tilde{S}_1^\top \otimes \Delta V^\top) \hat{\gamma}\|_2^2 + \|\theta_2^* - (D_2 \tilde{S}_2^\top \otimes \Delta V^\top) \hat{\gamma}\|_2^2,$$

and we have

$$\begin{aligned} \|\theta_1^* - (D_1 \tilde{S}_1^\top \otimes \Delta V^\top) \hat{\gamma}\|_2^2 &= \|\theta_1^* - (D_1 \tilde{S}_1^\top \otimes \Delta V^\top) (\tilde{S}_1 (\tilde{S}_1^\top \tilde{S}_1)^{-1} D_1^{-1} \otimes V \Delta^{-1}) \theta_1^*\|_2^2 \\ &= \|\theta_1^* - \left(D_1 \tilde{S}_1^\top \tilde{S}_1 (\tilde{S}_1^\top \tilde{S}_1)^{-1} D_1^{-1} \otimes \Delta V^\top V \Delta^{-1} \right) \theta_1^*\|_2^2 \\ &= \|\theta_1^* - \theta_1^*\|_2^2 \\ &= 0, \end{aligned}$$

and

$$\begin{aligned} &\|\theta_2^* - (D_2 \tilde{S}_2^\top \otimes \Delta V^\top) \hat{\gamma}\|_2 \\ &= \left\| \theta_2^* - \left(D_2 \tilde{S}_2^\top \tilde{S}_1 (\tilde{S}_1^\top \tilde{S}_1)^{-1} D_1^{-1} \otimes I_p \right) \theta_1^* \right\|_2 \\ &\leq \|\theta_2^*\|_2 + \left\| \left(D_2 \tilde{S}_2^\top \tilde{S}_1 (\tilde{S}_1^\top \tilde{S}_1)^{-1} D_1^{-1/2} D_1^{-1/2} \otimes \Delta^{1/2} \Delta^{-1/2} \right) \theta_1^* \right\|_2 \\ &= \|\theta_2^*\|_2 + \left\| \left(D_2 \tilde{S}_2^\top \tilde{S}_1 (\tilde{S}_1^\top \tilde{S}_1)^{-1} D_1^{-1/2} \otimes \Delta^{1/2} \right) \left(D_1^{-1/2} \otimes \Delta^{-1/2} \right) \theta_1^* \right\|_2 \\ &\leq \|\theta_2^*\|_2 + \left\| \left(D_2 \tilde{S}_2^\top \tilde{S}_1 (\tilde{S}_1^\top \tilde{S}_1)^{-1} D_1^{-1/2} \otimes \Delta^{1/2} \right) \right\|_{\text{op}} \left\| \left(D_1^{-1/2} \otimes \Delta^{-1/2} \right) \theta_1^* \right\|_2 \\ &= \|\theta_2^*\|_2 + \left\| D_2 \tilde{S}_2^\top \tilde{S}_1 (\tilde{S}_1^\top \tilde{S}_1)^{-1} D_1^{-1/2} \right\|_{\text{op}} \left\| \Delta^{1/2} \right\|_{\text{op}} \left\| \left(D_1^{-1/2} \otimes \Delta^{-1/2} \right) \theta_1^* \right\|_2 \\ &\leq \|\theta_2^*\|_2 + \left\| D_2^{1/2} \right\|_{\text{op}} \left\| \tilde{S}_2 D_2^{1/2} \right\|_{\text{op}} \left\| \tilde{S}_1 \right\|_{\text{op}} \left\| \left(\tilde{S}_1^\top \tilde{S}_1 \right)^{-1} \right\|_{\text{op}} \left\| D_1^{-1/2} \right\|_{\text{op}} \left\| \Delta^{1/2} \right\|_{\text{op}} \left\| \left(D_1^{-1/2} \otimes \Delta^{-1/2} \right) \theta_1^* \right\|_2. \end{aligned} \quad (23)$$

We now bound all terms involved in (23). Since $\|(D^{-1/2} \otimes \Delta^{-1/2}) \theta^*\|_2 \leq 1$, then $\|(D_1^{-1/2} \otimes \Delta^{-1/2}) \theta_1^*\|_2 \leq 1$ and,

$$\begin{aligned}
\|\theta_2^*\|_2^2 &= \sum_{i=1}^d \sum_{j=d_n+1}^n (\theta_{2ji}^*)^2 \\
&\leq \delta_n^2 \|M\|_{\text{op}} \sum_{i=1}^d \frac{1}{\Delta_{ii}} \sum_{j=d_n+1}^n \frac{(\theta_{2ji}^*)^2}{\lambda_j} \\
&\leq \delta_n^2 \|M\|_{\text{op}} \sum_{i=1}^d \sum_{j=1}^n \frac{(\theta_{2ji}^*)^2}{\lambda_j \Delta_{ii}} \\
&= \delta_n^2 \|M\|_{\text{op}} \left\| (D^{-1/2} \otimes \Delta^{-1/2}) \theta^* \right\|_2^2 \\
&\leq \delta_n^2 \|M\|_{\text{op}},
\end{aligned}$$

since $\lambda_j \leq \delta_n^2$, for all $j \geq d_n + 1$ and $\Delta_{ii} \leq \|M\|_{\text{op}}$ for all $1 \leq i \leq d$. Moreover, since $\|\tilde{S}_1^\top \tilde{S}_1 - I_{d_n}\|_{\text{op}} \leq \frac{1}{2}$, $\|\tilde{S}_1^\top \tilde{S}_1\|_{\text{op}} \leq \frac{3}{2}$, then $\|\tilde{S}_1\|_{\text{op}} \leq \sqrt{\frac{3}{2}}$. Besides, for all $x \in \mathbb{R}^{d_n}$ such that $\|x\|_2 = 1$, we have

$$|\|\tilde{S}_1^\top \tilde{S}_1 x\|_2 - 1| = |\|\tilde{S}_1^\top \tilde{S}_1 x\|_2 - \|x\|_2| \leq \left\| (\tilde{S}_1^\top \tilde{S}_1 - I_{d_n}) x \right\|_2 \leq \frac{1}{2},$$

Then, we obtain that $\|\tilde{S}_1^\top \tilde{S}_1 x\|_2 - 1 \geq -\frac{1}{2}$ and then $\|\tilde{S}_1^\top \tilde{S}_1 x\|_2 \geq \frac{1}{2}$, taking x the eigenvector of $\tilde{S}_1^\top \tilde{S}_1$ corresponding to its smallest eigenvalue, we obtain that $\|(\tilde{S}_1^\top \tilde{S}_1)^{-1}\|_{\text{op}}^{-1} \geq \frac{1}{2}$, and finally $\|(\tilde{S}_1^\top \tilde{S}_1)^{-1}\|_{\text{op}} \leq 2$. Moreover we have

$$\begin{aligned}
\|D_1^{-1/2}\|_{\text{op}} &\leq \frac{1}{\delta_n}, \\
\|D_2^{1/2}\|_{\text{op}} &\leq \delta_n, \\
\|\tilde{S}_2 D_2^{1/2}\|_{\text{op}} &\leq c\delta_n.
\end{aligned}$$

Thus,

$$\begin{aligned}
\left\| \theta_2^* - (D_2 \tilde{S}_2^\top \otimes \Delta V^\top) \hat{\gamma} \right\|_2 &\leq (\delta_n^2 \|M\|_{\text{op}})^{1/2} + \delta_n c \delta_n \left(\frac{3}{2}\right)^{1/2} 2 \frac{1}{\delta_n} \|M\|_{\text{op}}^{1/2} \\
&= (\delta_n^2 \|M\|_{\text{op}})^{1/2} (1 + c\sqrt{6})
\end{aligned}$$

Finally,

$$\left\| \theta^* - (D \tilde{S}^\top \otimes \Delta V^\top) \hat{\gamma} \right\|_2^2 \leq \delta_n^2 \|M\|_{\text{op}} (1 + c\sqrt{6})^2. \quad (24)$$

Furthermore, looking into the second term,

$$\begin{aligned}
\hat{\gamma}^\top \left(\tilde{S} D \tilde{S}^\top \otimes M \right) \hat{\gamma} &= \left\| \left(D^{1/2} \tilde{S}^\top \otimes \Delta^{1/2} V^\top \right) \hat{\gamma} \right\|_2^2 \\
&= \left\| \left(D_1^{1/2} \tilde{S}_1^\top \otimes \Delta^{1/2} V^\top \right) \hat{\gamma} \right\|_2^2 + \left\| \left(D_2^{1/2} \tilde{S}_2^\top \otimes \Delta^{1/2} V^\top \right) \hat{\gamma} \right\|_2^2 \\
&= \left\| \left(D_1^{-1/2} \otimes \Delta^{-1/2} \right) \theta_1^* \right\|_2^2 + \left\| \left(D_2^{1/2} \tilde{S}_2^\top \tilde{S}_1 \left(\tilde{S}_1^\top \tilde{S}_1 \right)^{-1} D_1^{-1} \otimes \Delta^{-1/2} \right) \theta_1^* \right\|_2^2 \\
&\leq 1 + \left\| \tilde{S}_2 D_2^{1/2} \right\|_{\text{op}}^2 \left\| \tilde{S}_1 \right\|_{\text{op}}^2 \left\| \left(\tilde{S}_1^\top \tilde{S}_1 \right)^{-1} \right\|_{\text{op}}^2 \left\| D_1^{-1/2} \right\|_{\text{op}}^2 \left\| \left(D_1^{-1/2} \otimes \Delta^{-1/2} \right) \theta_1^* \right\|_2^2 \\
&\leq 1 + c^2 \delta_n^2 \frac{3}{2} 4 \frac{1}{\delta_n^2} \\
&= 1 + 6c^2 \\
&= \left(1 + \sqrt{6}c \right)^2 - 2\sqrt{6}c \\
&\leq \left(1 + \sqrt{6}c \right)^2.
\end{aligned}$$

Finally, we obtain that

$$\left\| \theta^* - \left(D \tilde{S}^\top \otimes \Delta V^\top \right) \hat{\gamma} \right\|_2^2 + \lambda \hat{\gamma}^\top \left(\tilde{S} D \tilde{S}^\top \otimes M \right) \hat{\gamma} \leq \left(1 + \sqrt{6}c \right)^2 \left(\|M\|_{\text{op}} \delta_n^2 + \lambda \right), \quad (25)$$

and as a conclusion

$$\inf_{\Gamma \in \mathbb{R}^{s \times d}} \frac{1}{n} \|K S^\top \Gamma M - Z^*\|_F^2 + \lambda \text{Tr} \left(K S^\top \Gamma M \Gamma^\top S \right) \leq C^2 \left(\|M\|_{\text{op}} \delta_n^2 + \lambda \right), \quad (26)$$

where $C = 1 + \sqrt{6}c$. □

Now, as for the proof of Theorem 2, let us prove equation (11).

Proof. For any function in $\mathcal{B}(\mathcal{H}_K) = \{f \in \mathcal{H}_K : \|f\|_{\mathcal{H}_K} \leq 1\}$, Lemma 7 still holds, then

$$\mathbb{E} [l_f] \leq \mathbb{E}_n [l_f] + R_n(l \circ \mathcal{B}(\mathcal{H}_K)) + \sqrt{\frac{8 \log(2/\delta)}{n}}. \quad (27)$$

Then, using Corollary 1 from [51], we have that:

$$R_n(l \circ \mathcal{B}(\mathcal{H}_K)) \leq \sqrt{2} L \mathcal{R}_n(\mathcal{B}(\mathcal{H}_K)), \quad (28)$$

where

$$\begin{aligned}
\mathcal{R}_n(F) &= \mathbb{E} \left[\sup_{f \in F} \left| \frac{2}{n} \sum_{i=1}^n \sum_{j=1}^d \sigma_{ij} f(x_i)_j \right| \mid x_1, \dots, x_n \right] \\
&= \mathbb{E} \left[\sup_{f \in F} \left| \frac{2}{n} \sum_{i=1}^n \langle \sigma_i, f(x_i) \rangle_{\mathbb{R}^d} \right| \mid x_1, \dots, x_n \right],
\end{aligned}$$

where $\sigma_{11}, \dots, \sigma_{np}$ are nd independent Rademacher variables, and for all $1 \leq i \leq n$, $\sigma_i = (\sigma_{i1}, \dots, \sigma_{id})^\top$. Hence

$$\begin{aligned}
\mathcal{R}_n(\mathcal{B}(\mathcal{H}_\mathcal{K})) &= \mathbb{E} \left[\sup_{\|f\|_{\mathcal{H}_\mathcal{K}} \leq 1} \left| \frac{2}{n} \sum_{i=1}^n \langle \sigma_i, f(x_i) \rangle_{\mathbb{R}^d} \right| \mid x_1, \dots, x_n \right] \\
&= \mathbb{E} \left[\sup_{\|f\|_{\mathcal{H}_\mathcal{K}} \leq 1} \left| \left\langle \frac{2}{n} \sum_{i=1}^n \mathcal{K}_{x_i} \sigma_i, f \right\rangle_{\mathcal{H}_\mathcal{K}} \right| \mid x_1, \dots, x_n \right] \\
&\leq \frac{2}{n} \mathbb{E} \left[\left\| \sum_{i=1}^n \mathcal{K}_{x_i} \sigma_i \right\|_{\mathcal{H}_\mathcal{K}}^2 \mid x_1, \dots, x_n \right]^{1/2} \\
&= \frac{2}{n} \mathbb{E} \left[\sum_{i,j=1}^n \langle \sigma_i, \mathcal{K}(x_i, x_j) \sigma_j \rangle_{\mathbb{R}^d} \mid x_1, \dots, x_n \right]^{1/2} \\
&= \frac{2}{n} \mathbb{E} \left[\sum_{i,j=1}^n k(x_i, x_j) \langle \sigma_i, M \sigma_j \rangle_{\mathbb{R}^d} \mid x_1, \dots, x_n \right]^{1/2} \\
&= \frac{2}{n} \left(\sum_{i,j=1}^n k(x_i, x_j) \sum_{i',j'=1}^d \mathbb{E} [M_{i'j'} \sigma_{ii'} \sigma_{jj'} \mid x_1, \dots, x_n] \right)^{1/2} \\
&= \frac{2}{n} \left(\sum_{i=1}^n k(x_i, x_i) \sum_{i'=1}^d M_{i'i'} \right)^{1/2} \\
&= \frac{2}{n} (\text{Tr}(K \otimes M))^{1/2} \\
\mathcal{R}_n(\mathcal{B}(\mathcal{H}_\mathcal{K})) &\leq \frac{2}{n^{1/2}} \kappa^{1/2} \text{Tr}(M)^{1/2}.
\end{aligned}$$

Finally, for any function $f \in \mathcal{B}(\mathcal{H}_\mathcal{K})$, for all $\delta \in (0, 1)$, we have for a probability at least $1 - \delta$,

$$|\mathbb{E}[l_f] - \mathbb{E}_n[l_f]| \leq 4L \sqrt{\frac{2\kappa}{n} \text{Tr}(M)} + 2\sqrt{\frac{8 \log(2/\delta)}{n}}. \quad (29)$$

Now, for the approximation error term, we proceed as in the proof of Theorem 2. Let $\mathcal{H}_S = \left\{ f = \sum_{i=1}^n k(\cdot, x_i) M \left[S^\top \tilde{\Gamma} \right]_i \mid \gamma \in \mathbb{R}^{s \times d} \right\}$. By assumption 2 and Jensen's inequality,

$$\begin{aligned}
\mathbb{E}_n[l_{\tilde{f}_s}] - \mathbb{E}_n[l_{f_{\mathcal{H}_\mathcal{K}}}] &= \frac{1}{n} \sum_{i=1}^n l(\tilde{f}_s(x_i), y_i) - \frac{1}{n} \sum_{i=1}^n l(f_{\mathcal{H}_\mathcal{K}}(x_i), y_i) \\
&= \inf_{\substack{f \in \mathcal{H}_S \\ \|f\|_{\mathcal{H}_\mathcal{K}} \leq 1}} \frac{1}{n} \sum_{i=1}^n l(f(x_i), y_i) - \frac{1}{n} \sum_{i=1}^n l(f_{\mathcal{H}_\mathcal{K}}(x_i), y_i) \\
&\leq \inf_{\substack{f \in \mathcal{H}_S \\ \|f\|_{\mathcal{H}_\mathcal{K}} \leq 1}} \frac{L}{n} \sum_{i=1}^n \|f(x_i) - f_{\mathcal{H}_\mathcal{K}}(x_i)\|_2 \\
&\leq L \inf_{\substack{f \in \mathcal{H}_S \\ \|f\|_{\mathcal{H}_\mathcal{K}} \leq 1}} \sqrt{\frac{1}{n} \sum_{i=1}^n \|f(x_i) - f_{\mathcal{H}_\mathcal{K}}(x_i)\|_2^2} \\
&\leq L \inf_{\substack{f \in \mathcal{H}_S \\ \|f\|_{\mathcal{H}_\mathcal{K}} \leq 1}} \sqrt{\frac{1}{n} \|f^X - f_{\mathcal{H}_\mathcal{K}}^X\|_F^2},
\end{aligned}$$

where, for any $f \in \mathcal{H}_{\mathcal{K}}$, $f^X = (f(x_1), \dots, f(x_n))^\top \in \mathbb{R}^{n \times d}$. Let $\tilde{f}_s^R = \sum_{i=1}^n k(\cdot, x_i) M \left[S^\top \tilde{\Gamma}^R \right]_i$, where $\tilde{\Gamma}^R$ is a solution to

$$\inf_{\Gamma \in \mathbb{R}^{s \times d}} \frac{1}{n} \|KS^\top \Gamma M - f_{\mathcal{H}_{\mathcal{K}}}^X\|_F^2 + \lambda \text{Tr} (KS^\top \Gamma M \Gamma^\top S) .$$

It is easy to check that \tilde{f}_s^R is also a solution to

$$\inf_{\substack{f \in \mathcal{H}_S \\ \|f\|_{\mathcal{H}_{\mathcal{K}}} \leq \|\tilde{f}_s^R\|_{\mathcal{H}_{\mathcal{K}}}}} \frac{1}{n} \|f^X - f_{\mathcal{H}_{\mathcal{K}}}^X\|_F^2 .$$

Since we have $\|\tilde{f}_s^R\|_{\mathcal{H}_{\mathcal{K}}} \leq 1$ by Assumption 1, it holds

$$\begin{aligned} \inf_{\substack{f \in \mathcal{H}_S \\ \|f\|_{\mathcal{H}_{\mathcal{K}}} \leq 1}} \frac{1}{n} \|f^X - f_{\mathcal{H}_{\mathcal{K}}}^X\|_F^2 &\leq \inf_{\substack{f \in \mathcal{H}_S \\ \|f\|_{\mathcal{H}_{\mathcal{K}}} \leq \|\tilde{f}_s^R\|_{\mathcal{H}_{\mathcal{K}}}}} \frac{1}{n} \|f^X - f_{\mathcal{H}_{\mathcal{K}}}^X\|_F^2 \\ &= \inf_{\Gamma \in \mathbb{R}^{s \times d}} \frac{1}{n} \|KS^\top \Gamma M - f_{\mathcal{H}_{\mathcal{K}}}^X\|_F^2 + \lambda \text{Tr} (KS^\top \Gamma M \Gamma^\top S) . \end{aligned}$$

As a consequence, we have

$$\mathbb{E}_n[\ell_{\tilde{f}_s}] - \mathbb{E}_n[\ell_{f_{\mathcal{H}_k}}] \leq L \inf_{\Gamma \in \mathbb{R}^{s \times d}} \sqrt{\frac{1}{n} \|KS^\top \Gamma M - f_{\mathcal{H}_k}^X\|_F^2 + \lambda \text{Tr} (KS^\top \Gamma M \Gamma^\top S)} .$$

Finally, by Lemma 10 and Equation (29), we obtain the result stated. \square

Furthermore, we give the proof of the second claim, i.e. the excess risk bound for kernel ridge multi-output regression.

Proof. We now assume that the outputs are bounded, hence, without loss of generality, let assume $\mathcal{Y} \subset \mathcal{B}(\mathbb{R}^d)$. First, we prove Lipschitz-continuity of the square loss under Assumptions 1 and 3. Let $g : z \in \mathcal{H}_{\mathcal{K}}(\mathcal{X}) \mapsto \frac{1}{2} \|z - y\|_2^2$. We have that $\nabla g(z) = z - y$, and hence $\|\nabla g(z)\|_2 \leq \|f(x)\|_2 + 1$, for some $f \in \mathcal{H}_{\mathcal{K}}$ and $x \in \mathcal{X}$. By Assumptions 1 and 3 and Cauchy-Schwartz inequality, it is easy to check that

$$\|f(x)\|_2^2 \leq \left(\kappa \|M\|_{\text{op}} \|f(x)\|_2^2 \right)^{1/2} ,$$

which gives us that $\|f(x)\|_2 \leq \kappa^{1/2} \|M\|_{\text{op}}^{1/2}$ and then $\|\nabla g(z)\|_2 \leq \kappa^{1/2} \|M\|_{\text{op}}^{1/2} + 1$. We finally obtain that

$$|\ell(f(x), y) - \ell(f'(x'), y)| \leq \left(\kappa^{1/2} \|M\|_{\text{op}}^{1/2} + 1 \right) \|f(x) - f'(x')\|_2 .$$

We can then obtain the same generalisation bounds as above. Finally, looking at the approximation term,

$$\begin{aligned} \mathbb{E}_n[l_{\tilde{f}_s}] - \mathbb{E}_n[l_{f_{\mathcal{H}_k}}] &= \frac{1}{2n} \|\tilde{f}_s^X - Y\|_2^2 - \frac{1}{2n} \|f_{\mathcal{H}_k}^X - Y\|_2^2 \\ &\leq \frac{1}{2n} \|\tilde{f}_s^X - f_{\mathcal{H}_k}^X\|_2^2 \\ &\leq \inf_{\substack{f \in \mathcal{H}_S \\ \|f\|_{\mathcal{H}_k} \leq 1}} \frac{1}{2n} \|f^X - f_{\mathcal{H}_k}^X\|_2^2 \\ &\leq \inf_{\gamma \in \mathbb{R}^s} \frac{1}{n} \|KS^\top \gamma - f_{\mathcal{H}_k}^X\|_2^2 + \lambda \gamma^\top S K S^\top \gamma \\ &\leq C^2 (\lambda + \delta_n^2) . \end{aligned}$$

Here again, as in second claim of Theorem 2, we can directly use bound (20) and then, in combination with (29), we obtain the stated second claim in Theorem 4. \square

Finally, we here prove Lemma 9.

Proof. Let $f \in \mathcal{H}_{\mathcal{K}}$ such that $\|f\|_{\mathcal{H}_{\mathcal{K}}} \leq 1$ and $z = (f(x_1)^\top, \dots, f(x_n)^\top)^\top \in \mathbb{R}^{nd}$. We define the linear operator $S_X : \mathcal{H}_{\mathcal{K}} \rightarrow \mathbb{R}^{nd}$ such that $S_X(f) = (f(x_1)^\top, \dots, f(x_n)^\top)^\top$ for all $f \in \mathcal{H}_{\mathcal{K}}$. Then for all $f \in \mathcal{H}_{\mathcal{K}}$ and $z = (z_1^\top, \dots, z_n^\top)^\top \in \mathbb{R}^{nd}$ we have

$$\langle S_X(f), z \rangle_{\mathbb{R}^{nd}} = \sum_{i=1}^n \langle f(x_i), z_i \rangle_{\mathbb{R}^d} = \sum_{i=1}^n \langle f, \mathcal{K}_{x_i} z_i \rangle_{\mathcal{H}_{\mathcal{K}}} = \left\langle f, \sum_{i=1}^n \mathcal{K}_{x_i} z_i \right\rangle_{\mathcal{H}_{\mathcal{K}}} = \langle f, S_X^*(z) \rangle_{\mathcal{H}_{\mathcal{K}}}.$$

Hence

$$z^\top (K^{-1} \otimes M^{-1}) z = \left\langle (K \otimes M)^{-1} S_X(f), S_X(f) \right\rangle_{\mathbb{R}^{nd}} = \left\langle S_X^* \left((K \otimes M)^{-1} S_X(f) \right), f \right\rangle_{\mathcal{H}_{\mathcal{K}}}.$$

We recall the eigendecompositions of K and M

$$K = U (nD) U^\top = \sum_{i=1}^n n \lambda_i u_i u_i^\top$$

$$M = V \Delta V^\top = \sum_{j=1}^d \mu_j v_j v_j^\top.$$

Then,

$$\begin{aligned} K \otimes M &= \left(\sum_{i=1}^n n \lambda_i u_i u_i^\top \right) \otimes \left(\sum_{j=1}^d \mu_j v_j v_j^\top \right) \\ &= \sum_{i=1}^n \sum_{j=1}^d n \lambda_i \mu_j (u_i u_i^\top) \otimes (v_j v_j^\top) \\ &= \sum_{i=1}^n \sum_{j=1}^d n \lambda_i \mu_j (u_i) \otimes (v_j) (u_i^\top) \otimes (v_j^\top) \\ &= \sum_{i=1}^n \sum_{j=1}^d n \lambda_i \mu_j (u_i) \otimes (v_j) ((u_i) \otimes (v_j))^\top, \end{aligned}$$

and for all $1 \leq i, i' \leq n$ and $1 \leq j, j' \leq d$, if $(i, i') \neq (j, j')$, then $(u_i) \otimes (v_j)^\top ((u_{i'}) \otimes (v_{j'})) = 0$ and otherwise $(u_i) \otimes (v_j)^\top ((u_{i'}) \otimes (v_{j'})) = 1$. Then, this allows to show that the operator norm of a Kronecker product is the product of the operator norms, and that

$$(K \otimes M)^{-1} = \sum_{i=1}^n \sum_{j=1}^d (n \lambda_i \mu_j)^{-1} (u_i) \otimes (v_j) ((u_i) \otimes (v_j))^\top. \quad (30)$$

We define, for all $1 \leq i \leq n$ and $1 \leq j \leq d$,

$$\varphi_{ij} = \frac{1}{\sqrt{n \lambda_i \mu_j}} \sum_{l=1}^n u_{il} \mathcal{K}_{x_l} v_j. \quad (31)$$

By definition, $\text{span} \left((\varphi_{ij})_{1 \leq i \leq n, 1 \leq j \leq d} \right) \subset \text{span} \left((\mathcal{K}_{x_i} v_j)_{1 \leq i \leq n, 1 \leq j \leq d} \right)$ and we show that the φ_{ij} s are orthonormal,

$$\begin{aligned}
\langle \varphi_{ij}, \varphi_{i'j'} \rangle_{\mathcal{H}_{\mathcal{K}}} &= \left\langle \frac{1}{\sqrt{n\lambda_i\mu_j}} \sum_{l=1}^n u_{i_l} \mathcal{K}_{x_l} v_j, \frac{1}{\sqrt{n\lambda_{i'}\mu_{j'}}} \sum_{l'=1}^n u_{i'_{l'}} \mathcal{K}_{x_{l'}} v_{j'} \right\rangle_{\mathcal{H}_{\mathcal{K}}} \\
&= \frac{1}{\sqrt{n\lambda_i\mu_j}} \frac{1}{\sqrt{n\lambda_{i'}\mu_{j'}}} \sum_{l,l'}^n u_{i_l} u_{i'_{l'}} \langle \mathcal{K}_{x_l} v_j, \mathcal{K}_{x_{l'}} v_{j'} \rangle_{\mathcal{H}_{\mathcal{K}}} \\
&= \frac{1}{\sqrt{n\lambda_i\mu_j}} \frac{1}{\sqrt{n\lambda_{i'}\mu_{j'}}} \sum_{l,l'}^n u_{i_l} u_{i'_{l'}} \langle v_j, \mathcal{K}_{x_l, x_{l'}} v_{j'} \rangle_{\mathbb{R}^d} \\
&= \frac{1}{\sqrt{n\lambda_i\mu_j}} \frac{1}{\sqrt{n\lambda_{i'}\mu_{j'}}} \sum_{l,l'}^n u_{i_l} u_{i'_{l'}} k(x_l, x_{l'}) \langle v_j, M v_{j'} \rangle_{\mathbb{R}^d} \\
&= \frac{1}{\sqrt{n\lambda_i\mu_j}} \frac{1}{\sqrt{n\lambda_{i'}\mu_{j'}}} \sum_{l,l'}^n u_{i_l} u_{i'_{l'}} k(x_l, x_{l'}) \mu_{j'} \langle v_j, v_{j'} \rangle_{\mathbb{R}^d} \\
&= 0 \quad \text{if } j \neq j'.
\end{aligned}$$

Otherwise, if $j = j'$,

$$\begin{aligned}
\langle \varphi_{ij}, \varphi_{i'j'} \rangle_{\mathcal{H}_{\mathcal{K}}} &= \frac{1}{\sqrt{n\lambda_i}} \frac{1}{\sqrt{n\lambda_{i'}}} \sum_{l,l'}^n u_{i_l} u_{i'_{l'}} k(x_l, x_{l'}) \\
&= \frac{1}{\sqrt{n\lambda_i}} \frac{1}{\sqrt{n\lambda_{i'}}} \langle K u_i, u_{i'} \rangle_{\mathbb{R}^n} \\
&= \frac{1}{\sqrt{n\lambda_i}} \frac{1}{\sqrt{n\lambda_{i'}}} n \lambda_i \langle u_i, u_{i'} \rangle_{\mathbb{R}^n} \\
&= 0 \quad \text{if } i \neq i'.
\end{aligned}$$

Hence, $\langle \varphi_{ij}, \varphi_{i'j'} \rangle_{\mathcal{H}_{\mathcal{K}}} = 0$ if $(i, i') \neq (j, j')$ and if $(i, i') = (j, j')$,

$$\langle \varphi_{ij}, \varphi_{i'j'} \rangle_{\mathcal{H}_{\mathcal{K}}} = 1.$$

Finally, $\text{span} \left((\varphi_{ij})_{1 \leq i \leq n, 1 \leq j \leq d} \right) \subset \text{span} \left((\mathcal{K}_{x_i} v_j)_{1 \leq i \leq n, 1 \leq j \leq d} \right)$ and $\dim \left((\varphi_{ij})_{1 \leq i \leq n, 1 \leq j \leq d} \right) = nd = \dim \left((\mathcal{K}_{x_i} v_j)_{1 \leq i \leq n, 1 \leq j \leq d} \right)$, hence $(\varphi_{ij})_{1 \leq i \leq n, 1 \leq j \leq d}$ yields an orthonormal basis of $\text{span} \left((\mathcal{K}_{x_i} v_j)_{1 \leq i \leq n, 1 \leq j \leq d} \right)$. As a consequence, all $f \in \mathcal{H}_{\mathcal{K}}$ can be decomposed as $f = f_1 + f_2$, with $f_1 \in \text{span} \left((\mathcal{K}_{x_i} v_j)_{1 \leq i \leq n, 1 \leq j \leq d} \right)$ and

$f_2 \in \text{span} \left((\mathcal{K}_{x_i} v_j)_{1 \leq i \leq n, 1 \leq j \leq d} \right)^\perp$. Thus, for all $y \in \mathbb{R}^d$, y can be written as $y = \sum_{j=1}^d y_j v_j$ and

$$\begin{aligned}
\langle S_X(f), z \rangle_{\mathbb{R}^{nd}} &= \sum_{i=1}^n \langle f(x_i), z_i \rangle_{\mathbb{R}^d} \\
&= \sum_{i=1}^n \sum_{j=1}^d z_{ij} \langle f(x_i), v_j \rangle_{\mathbb{R}^d} \\
&= \sum_{i=1}^n \sum_{j=1}^d z_{ij} \langle f, \mathcal{K}_{x_i} v_j \rangle_{\mathcal{H}_K} \\
&= \sum_{i=1}^n \sum_{j=1}^d z_{ij} \langle f_1, \mathcal{K}_{x_i} v_j \rangle_{\mathcal{H}_K} + \sum_{i=1}^n \sum_{j=1}^d z_{ij} \langle f_2, \mathcal{K}_{x_i} v_j \rangle_{\mathcal{H}_K} \\
&= \sum_{i=1}^n \sum_{j=1}^d z_{ij} \langle f_1, \mathcal{K}_{x_i} v_j \rangle_{\mathcal{H}_K} \\
&= \langle S_X(f_1), z \rangle_{\mathbb{R}^{nd}}.
\end{aligned}$$

Hence, let $f \in \mathcal{H}_K$ such that $\|f\|_{\mathcal{H}_K} \leq 1$, written as $f = \sum_{i=1}^n \sum_{j=1}^d f_{ij} \varphi_{ij} + f^\perp$, with $f_{ij} \in \mathbb{R}$ for all $1 \leq i \leq n$ and $1 \leq j \leq d$ and such that $\sum_{i=1}^n \sum_{j=1}^d f_{ij}^2 \leq 1$ and $f^\perp \in \text{span} \left((\mathcal{K}_{x_i} v_j)_{1 \leq i \leq n, 1 \leq j \leq d} \right)^\perp$ such that $\|f^\perp\|_{\mathcal{H}_K} \leq 1$ (since $\|f\|_{\mathcal{H}_K} = \sum_{i=1}^n \sum_{j=1}^d f_{ij}^2 + \|f^\perp\|_{\mathcal{H}_K}^2 \leq 1$, we have that

$$S_X(f) = \sum_{i=1}^n \sum_{j=1}^d f_{ij} S_X(\varphi_{ij}),$$

and, for all $1 \leq l \leq n$,

$$\begin{aligned}
\varphi_{ij}(x_l) &= \frac{1}{\sqrt{n\lambda_i\mu_j}} \sum_{l'=1}^n u_{il'} k(x_{l'}, x_l) M v_j \\
&= \sqrt{\frac{\mu_j}{n\lambda_i}} K_{l:}^\top u_i v_j,
\end{aligned}$$

and then

$$S_X(\varphi_{ij}) = \sqrt{\frac{\mu_j}{n\lambda_i}} (K u_i) \otimes v_j = \sqrt{n\lambda_i\mu_j} u_i \otimes v_j. \quad (32)$$

Finally,

$$S_X(f) = \sum_{i=1}^n \sum_{j=1}^d f_{ij} (n\lambda_i\mu_j)^{1/2} u_i \otimes v_j. \quad (33)$$

Besides,

$$\begin{aligned}
(K \otimes M)^{-1} S_X(f) &= \left(\sum_{i=1}^n \sum_{j=1}^d (n\lambda_i\mu_i)^{-1} (u_i) \otimes (v_j) ((u_i) \otimes (v_j))^\top \right) \\
&\quad \times \left(\sum_{i'=1}^n \sum_{j'=1}^d f_{i'j'} (n\lambda_{i'}\mu_{j'})^{1/2} u_{i'} \otimes v_{j'} \right) \\
&= \sum_{i=1}^n \sum_{j=1}^d f_{ij} (n\lambda_i\mu_i)^{-1/2} u_i \otimes v_j.
\end{aligned}$$

Then,

$$\begin{aligned} S_X^* \left((K \otimes M)^{-1} S_X(f) \right) &= \sum_{i=1}^n \sum_{j=1}^d f_{ij} (n\lambda_i \mu_i)^{-1/2} S_X^* (u_i \otimes v_j) \\ &= \sum_{i=1}^n \sum_{j=1}^d f_{ij} (n\lambda_i \mu_i)^{-1/2} \sum_{i'=1}^n \mathcal{K}_{x_i}(u_{i'}, v_j), \end{aligned}$$

and finally,

$$\begin{aligned} \left\langle S_X^* \left((K \otimes M)^{-1} S_X(f) \right), f \right\rangle_{\mathcal{H}_K} &= \sum_{i,i'=1}^n \sum_{j,j'=1}^d \sum_{l=1}^n f_{ij} f_{i'j'} (n\lambda_i \mu_i)^{-1/2} u_{i_l} \langle \mathcal{K}_{x_l} v_j, \varphi_{i'j'} \rangle_{\mathcal{H}_K} \\ &= \sum_{i,i'=1}^n \sum_{j,j'=1}^d f_{ij} f_{i'j'} \left\langle (n\lambda_i \mu_i)^{-1/2} \sum_{l=1}^n u_{i_l} \mathcal{K}_{x_l} v_j, \varphi_{i'j'} \right\rangle_{\mathcal{H}_K} \\ &= \sum_{i,i'=1}^n \sum_{j,j'=1}^d f_{ij} f_{i'j'} \langle \varphi_{ij}, \varphi_{i'j'} \rangle_{\mathcal{H}_K} \\ &= \sum_{i=1}^n \sum_{j=1}^d f_{ij}^2 \\ \left\langle S_X^* \left((K \otimes M)^{-1} S_X(f) \right), f \right\rangle_{\mathcal{H}_K} &\leq 1. \end{aligned}$$

Thus, we do have the ellipse constraint

$$\| (K^{-1/2} \otimes M^{-1/2}) z \|_2 \leq 1. \quad (34)$$

□

A.4 Proof of Theorem 6

A.4.1 First claim of K-satisfiability

Let us now prove the first claim (left hand side of equation (4)) of the K-satisfiability for p -SR and p -SG sketches. It is articulated around the following two lemmas.

Lemma 11. *Let $M \in \mathbb{R}^{d \times d}$ be a symmetric matrix, $\varepsilon \in (0, 1)$, and \mathcal{C}_ε be an ε -cover of \mathcal{B}^d . Then we have*

$$\|M\|_{\text{op}} \leq \frac{1}{1 - 2\varepsilon - \varepsilon^2} \sup_{v \in \mathcal{C}_\varepsilon} |\langle v, Mv \rangle|.$$

Proof. Let M, ε and \mathcal{C}_ε as in Lemma 11. Let $u \in \mathcal{B}^d$. By definition, there exist $v \in \mathcal{C}_\varepsilon$ and $w \in \mathcal{B}^d$ such that $u = v + \varepsilon w$. We thus have

$$\langle u, Mu \rangle = \langle v, Mv \rangle + 2\varepsilon \langle v, Mw \rangle + \varepsilon^2 \langle w, Mw \rangle. \quad (35)$$

Taking the supremum on both sides of (35) we obtain

$$\begin{aligned} \sup_{u \in \mathcal{B}^d} |\langle u, Mu \rangle| &= \sup_{v \in \mathcal{C}_\varepsilon, w \in \mathcal{B}^d} \left(|\langle v, Mv \rangle| + 2\varepsilon |\langle v, Mw \rangle| + \varepsilon^2 |\langle w, Mw \rangle| \right) \\ &\leq \sup_{v \in \mathcal{C}_\varepsilon} |\langle v, Mv \rangle| + 2\varepsilon \sup_{v \in \mathcal{C}_\varepsilon, w \in \mathcal{B}^d} |\langle v, Mw \rangle| + \varepsilon^2 \sup_{w \in \mathcal{B}^d} |\langle w, Mw \rangle| \\ &\leq \sup_{v \in \mathcal{C}_\varepsilon} |\langle v, Mv \rangle| + 2\varepsilon \sup_{v' \in \mathcal{B}^d, w \in \mathcal{B}^d} |\langle v', Mw \rangle| + \varepsilon^2 \|M\|_{\text{op}} \\ &= \sup_{v \in \mathcal{C}_\varepsilon} |\langle v, Mv \rangle| + (2\varepsilon + \varepsilon^2) \|M\|_{\text{op}}, \end{aligned}$$

or again

$$\|M\|_{\text{op}} \leq \frac{1}{1 - 2\varepsilon - \varepsilon^2} \sup_{v \in \mathcal{C}_\varepsilon} |\langle v, Mv \rangle|.$$

□

Lemma 12. Let $S \in \mathbb{R}^{s \times n}$ be a p -SR or a p -SG sketch. Let $v \in \mathcal{B}^n$, then for every $t > 0$, we have

$$\mathbb{P} \left\{ \left| \|Sv\|_2^2 - \|v\|_2^2 \right| > \frac{4}{p} \sqrt{\frac{2t}{s}} + \frac{4t}{sp} \right\} \leq 2e^{-t}.$$

Proof. The proof of Lemma 12 is largely adapted from the proof of Theorem 2.13 in [13]. Let $S \in \mathbb{R}^{s \times n}$ be a p -SR or a p -SG sketch, and $v \in \mathcal{B}^n$. It is easy to check that for all $i \leq s$ we have $\mathbb{E} [Sv]_i^2 = \frac{1}{s} \|v\|_2^2$, such that

$$\left| \|Sv\|_2^2 - \|v\|_2^2 \right| = \left| \sum_{i=1}^s \left([Sv]_i^2 - \frac{1}{s} \|v\|_2^2 \right) \right|.$$

The proof then consists in applying Bernstein's inequality [13, Theorem 2.10] to the random variables $[Sv]_i^2$. We now have to find some constants ν and c such that $\sum_{i=1}^s \mathbb{E} [Sv]_i^4 \leq \nu$ and

$$\sum_{i=1}^s \mathbb{E} [Sv]_i^{2q} \leq \frac{q!}{2} \nu c^{q-2} \quad \text{for all } q \geq 3.$$

From (13) and (14), it is easy to check that the S_{ij} are independent and $1/(sp)$ sub-Gaussian. Then, for all $\lambda \in \mathbb{R}$, we have

$$\begin{aligned} \mathbb{E} [\exp(\lambda [Sv]_i)] &= \mathbb{E} \left[\exp \left(\lambda \sum_{j=1}^n S_{ij} v_j \right) \right] \\ &= \prod_{j=1}^n \mathbb{E} [\exp(\lambda S_{ij} v_j)] \\ &\leq \exp \left(\frac{\lambda^2}{2sp} \|v\|_2^2 \right) \\ &\leq \exp \left(\frac{\lambda^2}{2sp} \right). \end{aligned}$$

The random variable $[Sv]_i$ is therefore $1/(sp)$ sub-Gaussian, and Theorem 2.1 from [13] yields that for every integer $q \geq 2$ it holds

$$\mathbb{E} [Sv]_i^{2q} \leq \frac{q!}{2} 4 \left(\frac{2}{sp} \right)^q \leq \frac{q!}{2} \left(\frac{4}{sp} \right)^q.$$

Choosing $q = 2$, we obtain

$$\sum_{i=1}^s \mathbb{E} [Sv]_i^4 \leq \sum_{i=1}^s \left(\frac{4}{sp} \right)^2 = \frac{16}{sp^2},$$

such that we can choose $\nu = 16/(sp^2)$ and $c = 4/(sp)$. Applying Theorem 2.10 from [13] to the random variables $[Sv]_i^2$ finally gives that for any $t > 0$ it holds

$$\mathbb{P} \left\{ \left| \|Sv\|_2^2 - \|v\|_2^2 \right| > \frac{4}{p} \sqrt{\frac{2t}{s}} + \frac{4t}{sp} \right\} \leq 2e^{-t}.$$

□

Proof of the first claim of the K-satisfiability. Let $K \in \mathbb{R}^{n \times n}$ be a Gram matrix, and $S \in \mathbb{R}^{s \times n}$ be a p -SR or a p -SG sketch. Recall that we want to prove that there exists $c_0 > 0$ such that

$$\mathbb{P} \left\{ \|U_1^\top S^\top S U_1 - I_{d_n}\|_{\text{op}} > \frac{1}{2} \right\} \leq 2e^{-c_0 s},$$

where $K/n = UDU^\top$ is the SVD of K , and $U_1 \in \mathbb{R}^{n \times d_n}$ contains the left part of U . Let $\varepsilon \in (0, 1)$, and $\mathcal{C}_\varepsilon = \{v^1, \dots, v^{\mathcal{N}_\varepsilon}\}$ be an ε -cover of \mathcal{B}^{d_n} . We know that such a covering exists with cardinality $\mathcal{N}_\varepsilon \leq (1 + \frac{2}{\varepsilon})^{d_n}$, see e.g., [50]. Let $Q = U_1^\top S^\top S U_1 - I_{d_n}$, applying Lemma 11, we have

$$\begin{aligned} \mathbb{P} \left\{ \|Q\|_{\text{op}} > \frac{1}{2} \right\} &\leq \mathbb{P} \left\{ \sup_{i \leq \mathcal{N}_\varepsilon} |\langle v^i, Q v^i \rangle| > \frac{1 - 2\varepsilon - \varepsilon^2}{2} \right\} \\ &\leq \sum_{i \leq \mathcal{N}_\varepsilon} \mathbb{P} \left\{ |\langle v^i, Q v^i \rangle| > \frac{1 - 2\varepsilon - \varepsilon^2}{2} \right\} \\ &= \sum_{i \leq \mathcal{N}_\varepsilon} \mathbb{P} \left\{ \left| \|Sw^i\|_2^2 - \|w^i\|_2^2 \right| > \frac{1 - 2\varepsilon - \varepsilon^2}{2} \right\}, \end{aligned} \quad (36)$$

where $w^i = U_1 v^i \in \mathcal{B}^n$. Now, by Lemma 12, for any $w \in \mathcal{B}^n$, we have

$$\mathbb{P} \left\{ \left| \|Sw\|_2^2 - \|w\|_2^2 \right| > \frac{4}{p} \sqrt{\frac{2t}{s}} + \frac{4t}{sp} \right\} \leq 2e^{-t}.$$

Let $s \geq 32t/(\alpha^2 p^2)$, for some $\alpha \leq 1$. Then, we have $\frac{4}{p} \sqrt{\frac{2t}{s}} + \frac{4t}{sp} \leq \alpha + \frac{\alpha^2 p}{8} \leq 2\alpha$, and therefore

$$\mathbb{P} \left\{ \left| \|Sw\|_2^2 - \|w\|_2^2 \right| > 2\alpha \right\} \leq 2e^{-t}.$$

If we take $\alpha = (1 - 2\varepsilon - \varepsilon^2)/4$, we obtain

$$\mathbb{P} \left\{ \left| \|Sw\|_2^2 - \|w\|_2^2 \right| > \frac{1 - 2\varepsilon - \varepsilon^2}{2} \right\} \leq 2e^{-t}$$

as long as $s \geq \frac{512t}{p^2(1-2\varepsilon-\varepsilon^2)^2}$. Now, let $t = \frac{p^2(1-2\varepsilon-\varepsilon^2)^2}{1024} s + \log(\mathcal{N}_\varepsilon)$, and $s \geq 1024 \frac{\log(1+2/\varepsilon)}{p^2(1-2\varepsilon-\varepsilon^2)^2} d_n$. We do have

$$\frac{512t}{p^2(1-2\varepsilon-\varepsilon^2)^2} = \frac{s}{2} + \frac{512}{p^2(1-2\varepsilon-\varepsilon^2)^2} \log(\mathcal{N}_\varepsilon) \leq \frac{s}{2} + \frac{s}{2} = s,$$

such that

$$\mathbb{P} \left\{ \left| \|Sw\|_2^2 - \|w\|_2^2 \right| > \frac{1 - 2\varepsilon - \varepsilon^2}{2} \right\} \leq 2e^{-t} = \frac{2e^{-c_0 s}}{\mathcal{N}_\varepsilon},$$

where $c_0 = \frac{p^2(1-2\varepsilon-\varepsilon^2)}{1024}$. Plugging this result into (36), we get that as soon as $s \geq 1024 \frac{\log(1+2/\varepsilon)}{p^2(1-2\varepsilon-\varepsilon^2)^2} d_n$ it holds

$$\mathbb{P} \left\{ \|Q\|_{\text{op}} > \frac{1}{2} \right\} \leq 2e^{-c_0 s}.$$

Finally, we can tune ε to optimize the lower bound on s . If we take $\varepsilon = 0.1$, we obtain $s \geq 5120d_n/p^2$, and $c_0 \geq p^2/2560$. \square

A.4.2 Second claim of K-satisfiability

We now turn to the proof of the second claim (right hand side of equation (4)) of the K-satisfiability for p -SR and p -SG sketches. It builds upon the following two intermediate results, about the concentration of Lipschitz functions of Rademacher or Gaussian random variables.

Lemma 13. *Let $K > 0$, and let X_1, \dots, X_n be independent real random variables with $|X_i| \leq K$ for all $1 \leq i \leq n$. Let $F : \mathbb{R}^n \rightarrow \mathbb{R}$ be a L -Lipschitz convex function. Then, there exist $C, c > 0$ such that for any λ one has*

$$\mathbb{P}\{|F(X) - \mathbb{E} F(X)| \geq K\lambda\} \leq C' \exp(-c'\lambda^2/L^2).$$

Lemma 14. *Let X_1, \dots, X_n be i.i.d. standard Gaussian random variables. Let $F : \mathbb{R}^n \rightarrow \mathbb{R}$ be a L -Lipschitz function. Then, there exist $C, c > 0$ such that for any λ one has*

$$\mathbb{P}\{|F(X) - \mathbb{E} F(X)| \geq \lambda\} \leq C' \exp(-c'\lambda^2/L^2).$$

The above two lemmas are taken from [69], see Theorems 2.1.12 and 2.1.13 therein, but are actually well known results in the literature. In particular, Lemma 13 is adapted from Talagrand's inequality [68], while Lemma 14 is stated as Theorem 5.6 in [13], with explicit constants. We however choose the writing by [69] in order to be consistent with the Rademacher case.

Remark 3. Note that thanks to Lemma 13, we are even able to prove K -satisfiability for any sketch matrix S whose entries are i.i.d. centered and reduced bounded random variables.

Proof of the second claim of the K -satisfiability. Let $K \in \mathbb{R}^{n \times n}$ be a Gram matrix, and $S \in \mathbb{R}^{n \times s}$ be a p -SR or a p -SG sketch. Recall that we want to prove that there exist positive constants $c, c_1, c_2 > 0$ such that

$$\mathbb{P} \left\{ \|SU_2 D_2^{1/2}\|_{\text{op}} > c\delta_n \right\} \leq c_1 e^{-c_2 s},$$

where $K/n = UDU^\top$ is the SVD of K , $U_2 \in \mathbb{R}^{n \times (n-d_n)}$ is the right part of U , and $D_2 \in \mathbb{R}^{(n-d_n) \times (n-d_n)}$ is the right bottom part of D . Note that we have $SU_2 D_2^{1/2} = SU\bar{D}^{1/2}$, where $\bar{D} = \text{diag}(0_{d_n}, D_2) \in \mathbb{R}^{n \times n}$. Following [75], we have

$$\|SU\bar{D}^{1/2}\|_{\text{op}} = \sup_{u \in \mathcal{B}^s, v \in \mathcal{E}} |\langle u, Sv \rangle|,$$

where $\mathcal{E} = \{v \in \mathbb{R}^n : \exists w \in \mathcal{S}^{n-1}, v = U\bar{D}^{1/2}w\}$. Now, let $u^1, \dots, u^{\mathcal{N}}$ be a $1/2$ -cover of \mathcal{B}^s . We know that such a covering exists with cardinality $\mathcal{N} \leq 5^s$. We then have

$$\begin{aligned} \|SU\bar{D}^{1/2}\|_{\text{op}} &= \sup_{u \in \mathcal{B}^s, v \in \mathcal{E}} |\langle u, Sv \rangle| \\ &\leq \max_{i \leq \mathcal{N}} \sup_{v \in \mathcal{E}} |\langle u^i, Sv \rangle| + \frac{1}{2} \sup_{u \in \mathcal{B}^s, v \in \mathcal{E}} |\langle u, Sv \rangle| \\ &= \max_{i \leq \mathcal{N}} \sup_{v \in \mathcal{E}} |\langle u^i, Sv \rangle| + \frac{1}{2} \|SU\bar{D}^{1/2}\|_{\text{op}}, \end{aligned}$$

and rearranging implies that

$$\|SU\bar{D}^{1/2}\|_{\text{op}} \leq 2 \max_{i \leq \mathcal{N}} \sup_{v \in \mathcal{E}} |\langle u^i, Sv \rangle|.$$

Hence, for every $c > 0$ we have

$$\begin{aligned} \mathbb{P} \left(\|SU_2 D_2^{1/2}\|_{\text{op}} > c\delta_n \right) &\leq \mathbb{P} \left(\max_{i \leq \mathcal{N}} \sup_{v \in \mathcal{E}} |\langle u^i, Sv \rangle| > \frac{c}{2} \delta_n \right) \\ &\leq \sum_{i \leq \mathcal{N}} \mathbb{P} \left\{ \sup_{v \in \mathcal{E}} |\langle u^i, Sv \rangle| > \frac{c}{2} \delta_n \right\}. \end{aligned} \quad (37)$$

Now, recall that

$$S = \frac{1}{\sqrt{sp}} B \circ R,$$

where $B \in \mathbb{R}^{n \times s}$ is filled with i.i.d. Bernoulli random variables with parameter p , $R \in \mathbb{R}^{n \times s}$ is filled with i.i.d. Rademacher or Gaussian random variables for p -SR and p -SG sketches respectively, and \circ denotes the Hadamard (termwise) matrix product. The next step of the proof consists in controlling the right-hand side of (37) by showing that, conditionally on B , we have Lipschitz functions of Rademacher or Gaussian random variables, whose deviations can be bounded using Lemmas 13 and 14. Therefore, from now on we assume B to be fixed, and only consider the randomness with respect to R . Let $u \in \mathcal{B}^s$, and define $F: \mathbb{R}^{n \times s} \rightarrow \mathbb{R}$ as

$$F(R) = \frac{1}{\sqrt{sp}} \sup_{v \in \mathcal{E}} |\langle u, (B \circ R)v \rangle|.$$

It is direct to check that F is a convex function. Moreover, we have

$$\begin{aligned}
\sqrt{sp} F(R) &= \sup_{v \in \mathcal{E}} |\langle u, (B \circ R)v \rangle| \\
&= \sup_{v \in \mathcal{S}^{n-1}} |\langle u, (B \circ R)U\bar{D}^{1/2}v \rangle| \\
&= \sup_{v \in \mathcal{S}^{n-1}} |\langle \bar{D}^{1/2}U^\top (B \circ R)^\top u, v \rangle| \\
&= \left\| \bar{D}^{1/2}U^\top (B \circ R)^\top u \right\|_2.
\end{aligned}$$

Thus, for any R, R' we have

$$\begin{aligned}
\sqrt{sp} |F(R) - F(R')| &= \left| \left\| \bar{D}^{1/2}U^\top (B \circ R)^\top u \right\|_2 - \left\| \bar{D}^{1/2}U^\top (B \circ R')^\top u \right\|_2 \right| \\
&\leq \left\| \bar{D}^{1/2}U^\top (B \circ (R - R'))^\top u \right\|_2 \\
&\leq \left\| \bar{D}^{1/2} \right\|_{\text{op}} \|U^\top\|_{\text{op}} \|B \circ (R - R')\|_{\text{op}} \|u\|_2 \\
&\leq \delta_n \|B \circ (R - R')\|_F \\
&\leq \delta_n \|R - R'\|_F,
\end{aligned} \tag{38}$$

such that F is $\sqrt{\delta_n^2/(sp)}$ -Lipschitz. Moreover, we have

$$\begin{aligned}
\sqrt{sp} \mathbb{E}[F(R)] &= \mathbb{E} \left[\left\| D_2^{1/2}U_2^\top (B \circ R)^\top u \right\|_2 \right] \\
&\leq \sqrt{\mathbb{E} [u^\top (B \circ R)U_2 D_2 U_2^\top (B \circ R)^\top u]} \\
&= \sqrt{\sum_{k,k'=1}^s u_k u_{k'} \mathbb{E} [[(B \circ R)U_2 D_2 U_2^\top (B \circ R)^\top]_{kk'}]} \\
&= \sqrt{\sum_{k,k'=1}^s \sum_{l,l'=1}^n u_k u_{k'} [U_2 D_2 U_2^\top]_{ll'} \mathbb{E} [(B \circ R)_{kl} (B \circ R)_{k'l'}]} \\
&= \sqrt{\sum_{k=1}^s \sum_{l=1}^n B_{kl}^2 u_k^2 [U_2 D_2 U_2^\top]_{ll}} \\
&\leq \sqrt{\text{Tr}(D_2)},
\end{aligned}$$

which implies

$$\mathbb{E}[F(R)] \leq \sqrt{\frac{n}{sp}} \sqrt{\frac{\sum_{j=d_n+1}^n \lambda_j}{n}} \leq \sqrt{\frac{n}{sp}} \sqrt{\frac{1}{n} \sum_{j=d_n+1}^n \min(\lambda_j, \delta_n^2)} \leq \sqrt{\frac{\delta_n^2}{p}}, \tag{39}$$

where we have used the definition of δ_n^2 and the assumption $s \geq \delta_n^2 n$. Coming back to (37), we obtain

$$\begin{aligned}
\mathbb{P} \left\{ \|SU_2 D_2^{1/2}\|_{\text{op}} > c\delta_n \right\} &\leq 5^s \mathbb{E} \left[\mathbb{P} \left\{ \sup_{v \in \mathcal{E}} |\langle u, Sv \rangle| > \frac{c}{2} \delta_n \mid B \right\} \right] \\
&= 5^s \mathbb{E} \left[\mathbb{P} \left\{ F(R) > \frac{c}{2} \delta_n \right\} \right] \\
&\leq 5^s \mathbb{E} \left[\mathbb{P} \left\{ F(R) - \mathbb{E}[F(R)] > \delta_n \left(\frac{c}{2} - \frac{1}{\sqrt{p}} \right) \right\} \right] \tag{40}
\end{aligned}$$

$$\begin{aligned}
&\leq C 5^s \exp \left(-c' \left(\frac{c}{2} - \frac{1}{\sqrt{p}} \right)^2 \delta_n^2 \frac{sp}{\delta_n^2} \right) \tag{41} \\
&\leq C \exp \left(-c' \left(\left(\frac{c}{2} - \frac{1}{\sqrt{p}} \right)^2 p - \log(5) \right) s \right),
\end{aligned}$$

where (40) comes from the upper bound on $\mathbb{E}[F(R)]$ we derived in (39), and (41) derives from Lemmas 13 and 14 applied to the function F whose Lipschitz constant has been established in (38). Therefore, taking $c > 2\sqrt{\frac{\log(5)+1}{p}}$, we have

$$\mathbb{P}\left\{\|SU_2D_2^{1/2}\|_{\text{op}} > c\delta_n\right\} \leq c_1 e^{-c_2 s}$$

with $c_1 = C'$ and $c_2 = c' \left(\left(\frac{c}{2} - \frac{1}{\sqrt{p}} \right)^2 p - \log(5) \right) > 0$. \square

A.5 Proof of Proposition 5

We prove Proposition 5 thanks to duality properties.

Proof. Since problems (3) and (12) are convex problems under Slater's constraints, strong duality holds and we will show that they admit the same dual problem

$$\min_{\zeta \in \mathbb{R}^n} \sum_{i=1}^n \ell_i^*(-\zeta_i) + \frac{1}{2\lambda n} \zeta^\top KS^\top (SKS^\top)^\dagger SK\zeta. \quad (45)$$

First, we compute dual problem of (3), that can be rewritten

$$\begin{aligned} \min_{\gamma \in \mathbb{R}^s, u \in \mathbb{R}^n} \sum_{i=1}^n \ell_i(u_i) + \frac{\lambda n}{2} \gamma^\top SKS^\top \gamma \\ \text{s.t. } u = KS^\top \gamma. \end{aligned}$$

Therefore the Lagrangian writes

$$\begin{aligned} \mathcal{L}(\gamma, u, \zeta) &= \sum_{i=1}^n \ell_i(u_i) + \frac{\lambda n}{2} \gamma^\top SKS^\top \gamma + \sum_{i=1}^n \zeta_i(u_i - [KS^\top \gamma]_i) \\ &= \sum_{i=1}^n \ell_i(u_i) + \frac{\lambda n}{2} \gamma^\top SKS^\top \gamma + \sum_{i=1}^n \zeta_i u_i - \zeta^\top KS^\top \gamma. \end{aligned}$$

Differentiating with respect to γ and using the definition of the Fenchel-Legendre transform, one gets

$$\begin{aligned} g(\zeta) &= \inf_{\gamma \in \mathbb{R}^s, u \in \mathbb{R}^n} \mathcal{L}(\gamma, u, \zeta) \\ &= \sum_{i=1}^n \inf_{u_i \in \mathbb{R}} \{\ell_i(u_i) + \zeta_i u_i\} + \inf_{\gamma \in \mathbb{R}^s} \left\{ \frac{\lambda n}{2} \gamma^\top SKS^\top \gamma - \zeta^\top KS^\top \gamma \right\} \\ &= \sum_{i=1}^n -\ell_i^*(-\zeta_i) - \frac{1}{2\lambda n} \zeta^\top KS^\top (SKS^\top)^\dagger SK\zeta \end{aligned}$$

together with the equality $SKS^\top \tilde{\gamma} = \frac{1}{\lambda n} SK\tilde{\zeta}$, implying $\tilde{\gamma} = \frac{1}{\lambda n} (SKS^\top)^\dagger SK\tilde{\zeta}$, where $\tilde{\zeta} \in \mathbb{R}^n$ is the solution of the following dual problem

$$\min_{\beta \in \mathbb{R}^n} \sum_{i=1}^n \ell_i^*(-\beta_i) + \frac{1}{2\lambda n} \beta^\top KS^\top (SKS^\top)^\dagger SK\beta. \quad (45)$$

Then, we compute dual problem of (12), that can be rewritten

$$\begin{aligned} \min_{\omega \in \mathbb{R}^r, u \in \mathbb{R}^n} \sum_{i=1}^n \ell(u_i, y_i) + \frac{\lambda n}{2} \|\omega\|_2^2 \\ \text{s.t. } u = KS^\top \tilde{K}_r \omega. \end{aligned}$$

Therefore the Lagrangian writes

$$\begin{aligned} \mathcal{L}(\omega, u, \zeta) &= \sum_{i=1}^n \ell_i(u_i) + \frac{\lambda n}{2} \|\omega\|_2^2 + \sum_{i=1}^n \zeta_i(u_i - [KS^\top \tilde{K}_r \omega]_i) \\ &= \sum_{i=1}^n \ell_i(u_i) + \frac{\lambda n}{2} \|\omega\|_2^2 + \sum_{i=1}^n \zeta_i^\top u_i - \omega^\top \tilde{K}_r^\top SK\zeta. \end{aligned}$$

Differentiating with respect to ω and using the definition of the Fenchel-Legendre transform, one gets

$$\begin{aligned} g(\zeta) &= \inf_{\omega \in \mathbb{R}^r, u \in \mathbb{R}^n} \mathcal{L}(\omega, u, \zeta) \\ &= \sum_{i=1}^n \inf_{u_i \in \mathbb{R}} \{ \ell_i(u_i) + \zeta_i u_i \} + \inf_{\omega \in \mathbb{R}^r} \left\{ \frac{\lambda n}{2} \|\omega\|_2^2 - \omega^\top \tilde{K}^{-1/2^\top} SK\zeta \right\}. \end{aligned}$$

We have that

$$\begin{aligned} \frac{\partial}{\partial \omega} (\|\omega\|_2^2) &= 2\omega \\ \frac{\partial}{\partial \omega} (\omega^\top \tilde{K}_r^\top SK\zeta) &= \tilde{K}_r^\top SK\zeta, \end{aligned}$$

Then, setting the gradient to zero, we obtain

$$\tilde{\omega} = \frac{1}{\lambda n} \tilde{K}_r^\top SK\tilde{\zeta}. \quad (42)$$

Hence, putting it into the Lagrangian,

$$-\frac{1}{\lambda n} \zeta^\top KS^\top \tilde{K}^{-1/2} \tilde{K}_r^\top SK\zeta = -\frac{1}{\lambda n} KS^\top (SKS^\top)^\dagger SK\zeta,$$

and

$$\frac{1}{2\lambda n} \zeta^\top KS^\top \tilde{K}_r \tilde{K}_r^\top SK\zeta = \frac{1}{2\lambda n} KS^\top (SKS^\top)^\dagger SK\zeta.$$

Hence, $\tilde{\zeta} \in \mathbb{R}^n$ is the solution to the following dual problem

$$\min_{\beta \in \mathbb{R}^n} \sum_{i=1}^n \ell_i^*(-\beta_i) + \frac{1}{2\lambda n} \beta^\top KS^\top (SKS^\top)^\dagger SK\beta. \quad (45)$$

Finally, since both problems are convex and strong duality holds, we obtain through KKT conditions

$$\tilde{\omega} = (SKS^\top)^{-1/2^\top} (SKS^\top) \tilde{\gamma} = (\tilde{D}_r^{1/2} 0_{r \times s-r}) \tilde{V}^\top \tilde{\gamma}$$

and

$$\min_{\gamma \in \mathbb{R}^s} \frac{1}{n} \sum_{i=1}^n \ell([KS^\top \gamma]_i, y_i) + \frac{\lambda}{2} \gamma^\top SKS^\top \gamma = \min_{\omega \in \mathbb{R}^r} \sum_{i=1}^n \ell(\omega^\top \mathbf{z}_S(x_i), y_i) + \frac{\lambda}{2} \|\omega\|_2^2.$$

□

B Some background on statistical properties when using a p -sparsified sketch

In this section, we focus on p -sparsified sketches, and give, according to different standard choices of kernels (Gaussian, polynomial and first-order Sobolev), the different learning rates obtained for the excess risk as well as the condition on s .

We can first derive the following corollaries for the excess risk of p -sparsified sketched estimator in both single and multiple output settings.

Corollary 15. *For a p -sparsified sketch matrix S with $s \geq \max(C_0 d_n / p^2, \delta_n^2 n)$, we have with probability greater than $1 - C_1 e^{-sc(p)}$ in the single output setting,*

$$\mathbb{E} [\ell_{\tilde{f}_s}] \leq \mathbb{E} [\ell_{f_{\mathcal{H}_k}}] + LC \sqrt{\lambda + \delta_n^2} + 8L \sqrt{\frac{\kappa}{n}} + \mathcal{O} \left(\sqrt{\frac{s}{n}} \right), \quad (43)$$

and in the multiple output setting,

$$\mathbb{E} [\ell_{\tilde{f}_s}] \leq \mathbb{E} [\ell_{f_{\mathcal{H}_k}}] + LC \sqrt{\lambda + \|M\|_{\text{op}} \delta_n^2} + 8L \sqrt{\frac{\kappa \text{Tr}(M)}{n}} + \mathcal{O} \left(\sqrt{\frac{s}{n}} \right). \quad (44)$$

Table 3: Statistical dimension for different kernels.

Kernel	δ_n^2	d_n
Gaussian	$\mathcal{O}\left(\frac{\sqrt{\log(n)}}{n}\right)$	$\propto \sqrt{\log(n)}$
Polynomial	$\mathcal{O}\left(\frac{1}{n}\right)$	$\propto 1$
Sobolev	$\mathcal{O}\left(\frac{1}{n^{2/3}}\right)$	$\propto n^{1/3}$

Table 4: Learning rate obtained for excess risk and lower bound obtained on s for Gaussian sketching in worst case analysis.

Kernel	s	Learning rate
Gaussian	$\Omega\left(\sqrt{\log(n)}/p^2\right)$	$\mathcal{O}\left(\frac{(\log(n))^{1/4}}{n^{1/2}}\right)$
Polynomial	$\Omega\left(\frac{1}{p^2}\right)$	$\mathcal{O}\left(\frac{1}{\sqrt{n}}\right)$
Sobolev	$\Omega\left(n^{1/3}/p^2\right)$	$\mathcal{O}\left(\frac{1}{n^{1/3}}\right)$

We summarize the different behaviours of δ_n^2 and d_n in the different spectrum considered in Table 3 to get the exact condition on s at each time. More specifically, for a D th-order polynomial kernel, d_n , for any n is at most $D + 1$, leading to s of order $D + 1$ to be sufficient.

Finally, we can derive learning rate obtained as well as the exact condition on s for each scenario in Table 4. Compared with Random Fourier Features [47], we see that we obtain very slightly degraded learning rates for Gaussian and first-order Sobolev kernels in comparison with $\mathcal{O}(1/\sqrt{n})$, but they remain very close.

C Detailed algorithm of the generation and the decomposition of a p -sparsified sketch

In this section, we detail the process of generating a p -sparsified sketch and decomposing it as a product of a sub-Gaussian sketch S_{SG} and a sub-Sampling sketch S_{SS} .

Algorithm 1 Generation of a p -sparsified sketch

input : s, n and p

Generate a $s \times n$ matrix B whose entries are i.i.d. Bernoulli random variables of parameter p .

indices \leftarrow indices of non-null columns of B .

$B' \leftarrow B$ where all null columns have been deleted.

Generate a matrix M_{SG} of the same size as B' whose entries are either i.i.d. Gaussian or Rademacher random variables.

$S_{\text{SG}} \leftarrow M_{\text{SG}} \circ B'$, where \circ denotes the component-wise Hadamard matrix product.

return S_{SG} and indices

D Some background on per iteration complexity for single and multiple output regression

In this section, we detail the complexity in time and space of various matrix operations and iterations of stochastic subgradient descent in both single and multiple output settings for various sketching types.

We first recall the time and space complexities for elementary matrix products. The main advantage of using Sub-Sampling matrices is that computing SK is equivalent to sampling s training inputs and construct a $s \times n$ Gram matrix, hence we gain huge time complexity since we do not compute a matrix multiplication, as well as space complexity since we do not compute a $n \times n$ Gram matrix.

Table 5: Complexity of matrix operations for each sketching type.

Sketching type	Complexity type	SK	SKS^\top
Gaussian	time	$\mathcal{O}(n^2s)$	$\mathcal{O}(n^2s)$
	space	$\mathcal{O}(n^2)$	$\mathcal{O}(n^2)$
p -sparsified	time	$\mathcal{O}(nss')$	$\mathcal{O}(ss'^2)$
	space	$\mathcal{O}(ns')$	$\mathcal{O}(s'^2)$
Accumulation	time	$\mathcal{O}(nsm)$	$\mathcal{O}(s^2m^2)$
	space	$\mathcal{O}(ns)$	$\mathcal{O}(s^2)$
Sub-Sampling	time	$\mathcal{O}(ns)$	$\mathcal{O}(s^2)$
	space	$\mathcal{O}(ns)$	$\mathcal{O}(s^2)$

Table 6: Complexity of SGD iteration for each sketching type.

Sketching type	Complexity type	Single output	Multiple output
Gaussian	time	$\mathcal{O}(n^2s)$	$\mathcal{O}(n^2s)$
	space	$\mathcal{O}(n^2)$	$\mathcal{O}(n^2)$
p -sparsified	time	$\mathcal{O}(ss'^2)$	$\mathcal{O}(nss'd)$
	space	$\mathcal{O}(s'^2)$	$\mathcal{O}(ns')$
Accumulation	time	$\mathcal{O}(s^2m^2)$	$\mathcal{O}(nsm d)$
	space	$\mathcal{O}(s^2)$	$\mathcal{O}(ns)$
Sub-Sampling	time	$\mathcal{O}(s^3)$	$\mathcal{O}(nsd)$
	space	$\mathcal{O}(s^2)$	$\mathcal{O}(ns)$

As a consequence, the main advantage of our p -sparsified sketches is their ability to be decomposed as $S = S_{\text{SG}}S_{\text{SS}}$, where $S_{\text{SG}} \in \mathbb{R}^{s \times s'}$ is a sparse sub-Gaussian sketch and $S_{\text{SS}} \in \mathbb{R}^{s' \times n}$ is a sub-Sampling sketch, as explained in Section 3 and Appendix C. We recall that Accumulation matrices from [20] writes as $S = \sum_{i=1}^m S_{(i)}$, where the $S_{(i)}$ s are sub-sampling matrices whose each row is multiplied by independent Rademacher variables. Hence, both p -sparsified and Accumulation sketches are interesting since it completely benefits from computational efficiency of sub-sampling matrices. See table 5 for complexity analysis of matrix multiplications.

Going into the per iteration of SGD algorithm, the main difference between single and multiple output settings are the computation of feature maps, relying on the construction of SKS^\top and the computation of the square root of its pseudo-inverse, for the single output setting which is not present in the multiple output settings, and the presence of M in the multiple output setting. We assume in our framework that d and even d^2 are typically very small in comparison with n . Hence, following the computation of gradients and Jacobian matrices (in multiple output case), we report all complexities in Table 6. We see that from a time complexity perspective, p -sparsified sketches outperform Accumulation sketches in single output settings as long as $s' \leq \sqrt{sm}$, and in multiple output settings as long as $s' \leq m$. From a space complexity perspective, Accumulation is always better as s' is typically greater than s , otherwise it shows poor performance. However, p is usually chosen such that s' is not very large compared with s .

E Discussion with dual implementation

In this section we detail the discussion about duality of kernel machines when using sketching. A first idea consists in computing the dual problem to the sketched problem (3). It writes

$$\min_{\zeta \in \mathbb{R}^n} \sum_{i=1}^n \ell_i^*(-\zeta_i) + \frac{1}{2\lambda n} \zeta^\top K S^\top (S K S^\top)^\dagger S K \zeta, \quad (45)$$

where $\ell_i = \ell(\cdot, y_i)$, and f^* denotes the Fenchel-Legendre transform of f , such that $f^*(\theta) = \sup_x \langle \theta, x \rangle - f(x)$. First note that sketching with a subsampling matrix in the primal is thus equivalent to using a Nystrom approximation in the dual. This remark generalizes for any loss function the

observation made in [75] for the kernel Ridge regression. However, although the ℓ_i^* might be easier to optimize, solving (45) seems not a meaningful option, as duality brought us back to optimizing over \mathbb{R}^n , what we initially intended to avoid. The natural alternative thus appears to use duality first, and then sketching. The resulting problem writes

$$\min_{\theta \in \mathbb{R}^s} \sum_{i=1}^n \ell_i^* (-[S^\top \theta]_i) + \frac{1}{2\lambda n} \theta^\top S K S^\top \theta. \quad (46)$$

It is interesting to note that (46) is also the sketched version of Problem (45), which we recall is itself the dual to the sketched primal problem. Hence, sketching in the dual can be seen as a double approximation. As a consequence, the objective value reached by minimizing (46) is always larger than that achieved by minimizing (3), and theoretical guarantees for such an approach are likely to be harder to obtain. Another limitation of (46) regards the $\ell_i^* (-[S^\top \theta]_i)$. Indeed, these terms generally contain the non-differentiable part of the objective function (for the ϵ -insensitive Ridge regression we have $\sum_i \ell_i^*(\theta_i) = \frac{1}{2} \|\theta\|_2^2 + \langle \theta, y \rangle + \epsilon \|\theta\|_1$ for instance), and are usually minimized by proximal gradient descent. However, using a similar approach for (46) is impossible, since the proximal operator of $\ell_i^*(S^\top \cdot)$ is only computable if $S^\top S = I_n$, which is never the case. Instead, one may use a primal-dual algorithm [18, 70, 22], which solves the saddle-point optimization problem of the Lagrangian, but maintain a dual variable in \mathbb{R}^n . Coordinate descent versions of such algorithms [28, 2] may also be considered, as they leverage the possible sparsity of S to reduce the per-iteration cost. In order to converge, these algorithms however require a number of iteration that is of the order of n , making them hardly relevant in the large scale setting we consider.

For all the reasons listed above, we thus believe that minimizing (45) or (46) is not theoretically relevant nor computationally attractive, and that running stochastic (sub-)gradient descent on the primal problem, as detailed at the beginning of the section, is the best way to proceed algorithmically despite the possibly more elegant dual formulations. Finally, we highlight that although the condition $S^\top S = I_n$ is almost surely not verified (we have $S \in \mathbb{R}^{s \times n}$ with $s < n$), we still have $\mathbb{E}[S^\top S] = I_N$ for most sketching matrices. An interesting research direction could thus consist in running a proximal gradient descent assuming that $S^\top S = I_n$, and controlling the error incurred by such an approximation.

F Examples of Lipschitz-continuous losses

Robust losses for multiple output regression: For $p \geq 1$, $\mathcal{Y} \subset \mathbb{R}^p$, and for all $y, y' \in \mathcal{Y}$, $\ell(y, y') = g(y - y')$, where g is:

For κ -Huber: For $\kappa > 0$:

$$\forall y \in \mathcal{Y}, g(y) = \begin{cases} \frac{1}{2} \|y\|_{\mathcal{Y}}^2 & \text{if } \|y\|_{\mathcal{Y}} \leq \kappa \\ \kappa (\|y\|_{\mathcal{Y}} - \frac{\kappa}{2}) & \text{otherwise} \end{cases}.$$

For ϵ -SVR (i.e. ϵ -insensitive ℓ_1 loss): For $\epsilon > 0$:

$$\forall y \in \mathcal{Y}, g(y) = \begin{cases} \|y\|_{\mathcal{Y}} - \epsilon & \text{if } \|y\|_{\mathcal{Y}} \geq \epsilon \\ 0 & \text{otherwise} \end{cases}.$$

The pinball loss [39] for joint quantile regression: For d quantile levels, $\tau_1 < \tau_2 < \dots < \tau_d$ with $\tau_i \in (0, 1)$, we define:

$$\ell_\tau(f(x), y) = L_\tau(f(x) - y \mathbf{1}_d),$$

with the following definition for L_τ the extension of pinball loss to \mathbb{R}^d [60]:
For $r \in \mathbb{R}^d$:

$$L_\tau(r) = \sum_{j=1}^d \begin{cases} \tau_j r_j & \text{if } r_j \geq 0, \\ (\tau_j - 1) r_j & \text{if } r_j < 0. \end{cases}$$

G Additional experiments

In this section, we bring some additional experiments and details.

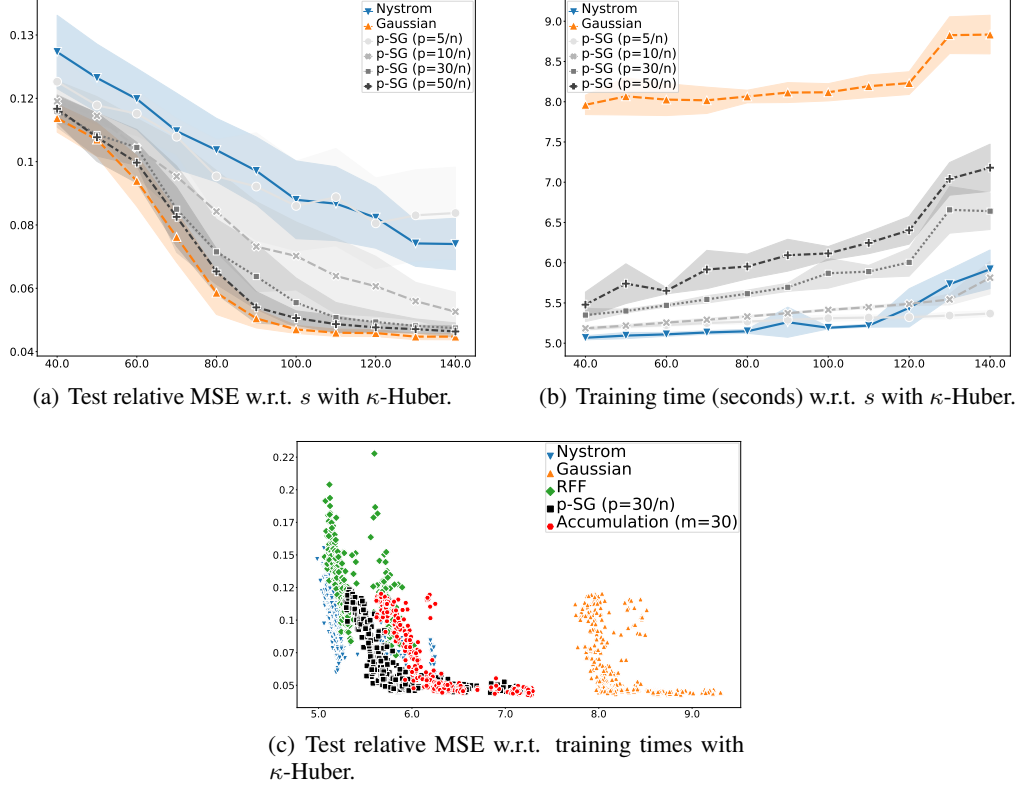


Figure 2: Trade-off between Accuracy and Efficiency for p -SG sketches with κ -Huber loss.

Table 7: Numbers of training samples (n_{tr}), test samples (n_{te}), features (q) and targets (d).

Dataset	n_{tr}	n_{te}	q	d
Boston	354	152	13	5
otoliths	3780	165	4096	5
rf1	4108	5017	64	8
rf2	4108	5017	576	8
scm1d	8145	1658	280	16
scm20d	7463	1503	61	16

G.1 Simulated dataset for single output regression

First, we report the plots obtained with κ -Huber for p -SG sketches (see Figure 2) and note that we observe a behaviour similar to p -SR sketches when varying p and in comparison to other types of sketching and RFFs. However, we see that the MSE obtained is slightly worse than p -SR sketches. An explanation might be that, in a very sparse regime, i.e. very low p , a p -SG sketch is too different than a Gaussian sketch, making it lose some good statistical properties of Gaussian sketches. We however observe that the larger p is, the smaller is the statistical performance between p -SR and p -SG sketches.

We then report in the following the corresponding plots obtained with ϵ -SVR, that witnesses the same phenomenon observed earlier with κ -Huber about the interpolation between Nyström method and Gaussian sketching while varying the probability of being different than 0 p , with p -SR sketches (see Figure 3) and p -SG sketches (see Figure 4).

G.2 Multi-Output Regression on real datasets

We here first a brief presentation on River Flow and Supply Chain Management:

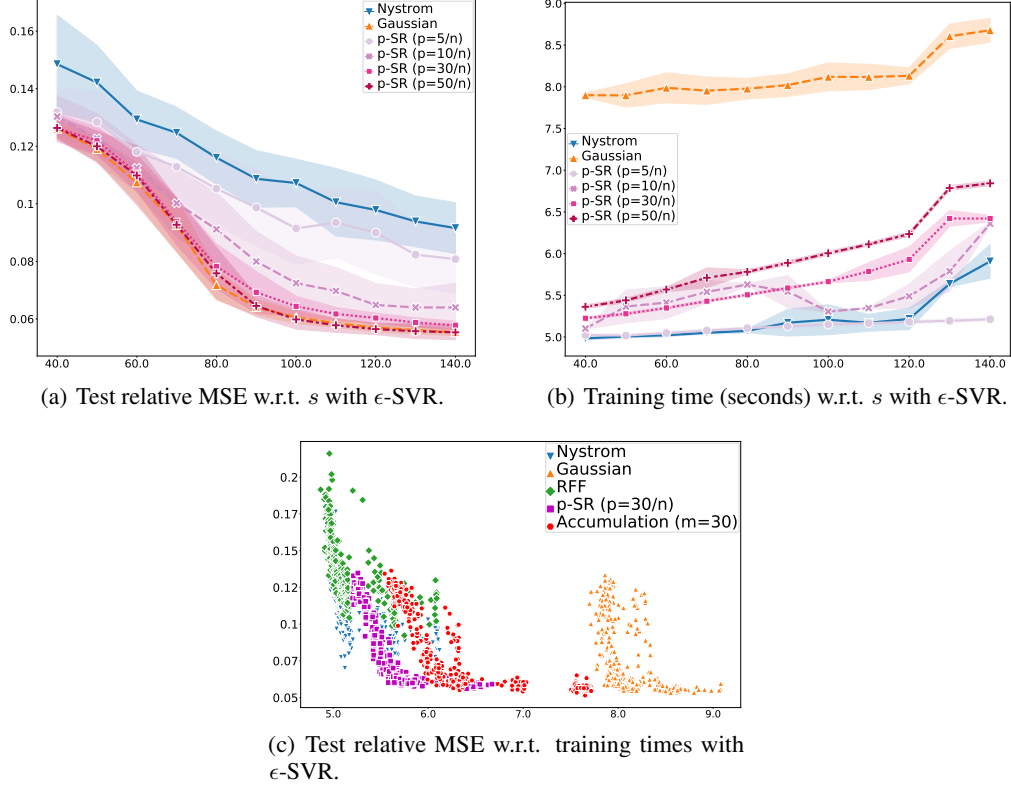


Figure 3: Trade-off between Accuracy and Efficiency for p -SR sketches with ϵ -SVR problem.

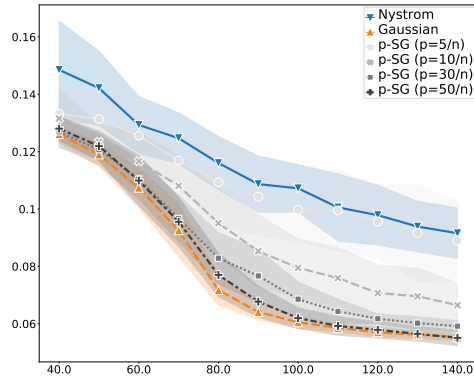
1. River Flow datasets aim at predicting the river network flows for 48 hours in the future at specific locations. These locations are 8 sites in the Mississippi River network in the United States and were obtained from the US National Weather Service. Dataset rf2 extends rf1 since it contains additional precipitation forecast information for each of the 8 sites.
2. The datasets scm1d and scm20d come from the Trading Agent Competition in Supply Chain Management (TAC SCM) tournament from 2010. More details about data preprocessing can be found in [32]. The dataset contains prices of products at specific days, and the task is to predict to the next day mean price (scm1d) or mean price for 20-days in the future (scm20d) for each product in the simulation.

To conduct these experiments, the train-test splits used are the ones available at <http://mulan.sourceforge.net/datasets-mtr.html>. Besides, we used multi-output Kernel Ridge Regression framework and an input Gaussian kernel of σ^2 and an operator $M = I_d$. We selected regularisation parameter λ and bandwidth of kernel σ^2 via a 5-fold cross-validation. Results are averages over 30 replicates for sketched models.

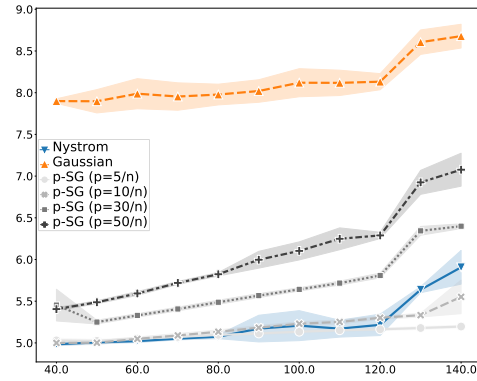
We compare our non-sketched framework with the sketched one, and we furthermore compare our p -sparsified sketches with Accumulation sketch from [20]. Moreover, we report the range of results obtained by SOTA methods available at [63]. All results in terms of Test RRMSE are reported in Table 8, we see that our p -sparsified sketches allow to ally statistical and computational performance, since we maintain an accuracy of the same order as without sketching, and these sketches outperform Accumulation in terms of training times (see Table 2). In comparison to SOTA, our framework does not compete with the best results obtained in [63], but almost always remains within the range of results obtained with SOTA methods.

Table 8: Test RRMSE and ARRME for different methods on the MTR datasets. For decomposable kernel-based models, loss here is square loss and $s = 200$ when performing Sketching.

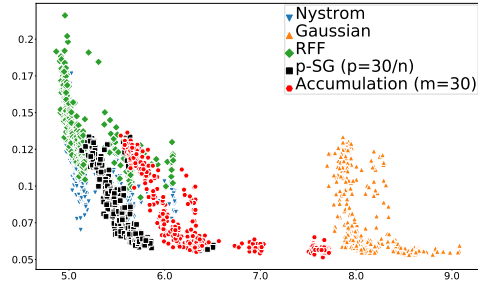
Dataset	Targets	w/o Sketch	$20/n_{tr}$ -SR	$20/n_{tr}$ -SG	Acc. $m = 20$	Results in [63]
rf1	Mean	0.575	0.582 ± 0.002	0.583 ± 0.002	0.575 ± 0.0002	[0.091, 0.983]
	chsi2	0.351	0.357 ± 0.003	0.359 ± 0.002	0.351 ± 0.001	[0.033, 0.797]
	nasi2	1.085	1.128 ± 0.002	1.128 ± 0.003	1.110 ± 0.0001	[0.376, 1.951]
	eadm7	0.388	0.398 ± 0.002	0.400 ± 0.002	0.388 ± 0.001	[0.039, 1.019]
	sclm7	0.660	0.661 ± 0.003	0.663 ± 0.004	0.650 ± 0.001	[0.047, 1.503]
	clkm7	0.283	0.281 ± 0.001	0.282 ± 0.001	0.281 ± 0.0003	[0.031, 0.587]
	vali2	0.614	0.635 ± 0.006	0.637 ± 0.006	0.612 ± 0.002	[0.037, 0.571]
	napm7	0.593	0.603 ± 0.012	0.602 ± 0.001	0.598 ± 0.001	[0.038, 0.909]
	dldi4	0.629	0.595 ± 0.002	0.595 ± 0.002	0.614 ± 0.001	[0.029, 0.534]
rf2	Mean	0.578	0.629 ± 0.003	0.628 ± 0.002	0.627 ± 0.003	[0.095, 1.103]
	chsi2	0.318	0.348 ± 0.004	0.349 ± 0.003	0.343 ± 0.006	[0.034, 0.737]
	nasi2	1.075	1.086 ± 0.002	1.062 ± 0.002	1.097 ± 0.003	[0.384, 3.143]
	eadm7	0.339	0.357 ± 0.003	0.355 ± 0.002	0.355 ± 0.005	[0.040, 0.737]
	sclm7	0.601	0.658 ± 0.009	0.667 ± 0.008	0.642 ± 0.010	[0.049, 0.970]
	clkm7	0.327	0.317 ± 0.003	0.340 ± 0.002	0.312 ± 0.003	[0.041, 0.891]
	vali2	0.699	0.840 ± 0.018	0.836 ± 0.013	0.836 ± 0.016	[0.047, 0.956]
	napm7	0.599	0.751 ± 0.007	0.722 ± 0.005	0.761 ± 0.010	[0.039, 0.617]
	dldi4	0.670	0.673 ± 0.004	0.695 ± 0.002	0.665 ± 0.004	[0.032, 0.770]
scm1d	Mean	0.419	0.418 ± 0.0002	0.419 ± 0.0001	0.420 ± 0.0003	[0.330, 0.457]
	lbl	0.359	0.360 ± 0.0003	0.359 ± 0.0003	0.361 ± 0.0004	[0.294, 0.409]
	mtlp2	0.353	0.353 ± 0.0004	0.353 ± 0.0003	0.355 ± 0.0004	[0.308, 0.436]
	mtlp3	0.409	0.411 ± 0.0003	0.411 ± 0.0004	0.411 ± 0.0004	[0.315, 0.442]
	mtlp4	0.417	0.420 ± 0.0005	0.419 ± 0.0005	0.419 ± 0.0006	[0.325, 0.461]
	mtlp5	0.499	0.494 ± 0.0005	0.495 ± 0.0006	0.499 ± 0.0009	[0.349, 0.530]
	mtlp6	0.538	0.533 ± 0.0006	0.533 ± 0.0005	0.537 ± 0.0007	[0.347, 0.540]
	mtlp7	0.534	0.529 ± 0.0006	0.529 ± 0.0006	0.533 ± 0.0008	[0.338, 0.526]
	mtlp8	0.545	0.541 ± 0.0009	0.541 ± 0.0008	0.545 ± 0.0010	[0.345, 0.504]
	mtlp9	0.384	0.386 ± 0.0004	0.386 ± 0.0003	0.386 ± 0.0006	[0.323, 0.456]
	mtlp10	0.388	0.389 ± 0.0004	0.390 ± 0.0004	0.389 ± 0.0006	[0.339, 0.456]
	mtlp11	0.424	0.424 ± 0.0004	0.424 ± 0.0004	0.424 ± 0.0004	[0.327, 0.445]
	mtlp12	0.423	0.420 ± 0.0004	0.420 ± 0.0003	0.422 ± 0.0005	[0.350, 0.466]
	mtlp13	0.347	0.350 ± 0.0004	0.350 ± 0.0003	0.348 ± 0.0005	[0.322, 0.419]
	mtlp14	0.345	0.349 ± 0.0005	0.349 ± 0.0004	0.346 ± 0.0004	[0.356, 0.472]
	mtlp15	0.360	0.361 ± 0.0003	0.361 ± 0.0003	0.361 ± 0.0003	[0.314, 0.406]
	mtlp16	0.375	0.376 ± 0.0003	0.376 ± 0.0003	0.375 ± 0.0004	[0.322, 0.407]
scm20d	Mean	0.751	0.753 ± 0.001	0.752 ± 0.001	0.752 ± 0.001	[0.394, 0.763]
	lbl	0.612	0.617 ± 0.003	0.616 ± 0.003	0.613 ± 0.001	[0.356, 0.678]
	mtlp2a	0.630	0.634 ± 0.004	0.632 ± 0.003	0.630 ± 0.001	[0.352, 0.688]
	mtlp3a	0.603	0.609 ± 0.003	0.607 ± 0.002	0.603 ± 0.001	[0.363, 0.683]
	mtlp4a	0.640	0.649 ± 0.003	0.645 ± 0.003	0.638 ± 0.002	[0.374, 0.730]
	mtlp5a	0.978	0.973 ± 0.011	0.974 ± 0.011	0.976 ± 0.007	[0.413, 0.846]
	mtlp6a	0.992	0.994 ± 0.012	0.994 ± 0.013	0.987 ± 0.007	[0.424, 0.843]
	mtlp7a	1.000	1.000 ± 0.012	1.004 ± 0.013	1.001 ± 0.008	[0.404, 0.833]
	mtlp8a	0.999	1.002 ± 0.014	1.004 ± 0.016	1.000 ± 0.009	[0.407, 0.851]
	mtlp9a	0.696	0.699 ± 0.003	0.699 ± 0.004	0.701 ± 0.001	[0.382, 0.737]
	mtlp10a	0.718	0.717 ± 0.003	0.716 ± 0.004	0.719 ± 0.002	[0.413, 0.753]
	mtlp11a	0.723	0.727 ± 0.003	0.725 ± 0.002	0.726 ± 0.001	[0.402, 0.769]
	mtlp12a	0.716	0.713 ± 0.005	0.712 ± 0.005	0.714 ± 0.005	[0.429, 0.787]
	mtlp13a	0.699	0.700 ± 0.007	0.698 ± 0.005	0.701 ± 0.003	[0.400, 0.751]
	mtlp14a	0.671	0.670 ± 0.005	0.668 ± 0.003	0.673 ± 0.002	[0.411, 0.779]
	mtlp15a	0.670	0.667 ± 0.006	0.667 ± 0.003	0.674 ± 0.002	[0.384, 0.727]
	mtlp16a	0.676	0.674 ± 0.007	0.672 ± 0.004	0.678 ± 0.003	[0.386, 0.754]



(a) Test relative MSE w.r.t. s with ϵ -SVR.



(b) Training time (seconds) w.r.t. s with ϵ -SVR.



(c) Test relative MSE w.r.t. training times with ϵ -SVR.

Figure 4: Trade-off between Accuracy and Efficiency for p -SG sketches with ϵ -SVR problem.